Meteoritics & Planetary Science 33, 1065–1085 (1998)

Progressive alteration in CV3 chondrites: More evidence for asteroidal alteration

ALEXANDER N. KROT[1]*, MICHAEL I. PETAEV[2], EDWARD R. D. SCOTT[1†], BYEON-GAK CHOI[3,4], MICHAEL E. ZOLENSKY[5] AND KLAUS KEIL[1†]

[1]Hawai'i Institute of Geophysics and Planetology, School of Ocean and Earth Science and Technology, University of Hawai'i at Manoa, Honolulu, Hawai'i 96822, USA
[2]Harvard-Smithsonian Center for Astrophysics, Cambridge Massachusetts, USA
[3]Department of Earth and Planetary Sciences, University of California, Los Angeles, California 90095-1567, USA
[4]Institute of Geophysics and Planetary Physics, University of California, Los Angeles, California 90095-1567, USA
[5]Earth Science and Solar System Exploration Division, NASA, Johnson Space Center, Houston, Texas 77058, USA
[†]Also associated with the Hawai'i Center for Volcanology
*Correspondence author's e-mail address: sasha@pgd.hawaii.edu

(Received 1997 September 15; accepted in revised form 1998 February 9)
(Presented at the Workshop on Parent Body and Nebular Modification of Chondritic Materials at the University of Hawaii, Maui, Hawaii, USA 1997 July 16–19)

Abstract–The oxidized CV3 chondrites can be divided into two major subgroups or lithologies, Bali-like ($CV3_{oxB}$) and Allende-like ($CV3_{oxA}$), in which chondrules, calcium-aluminum-rich inclusions (CAIs) and matrices show characteristic alteration features (Weisberg *et al.*, 1997; Krot *et al.*, 1997d; Kimura and Ikeda, 1997). The $CV3_{oxB}$ lithology is present in Bali, Kaba, parts of the Mokoia breccia and, possibly, in Grosnaja and Allan Hills (ALH) 85006. It is characterized by the presence of the secondary low-Ca phyllosilicates (saponite and sodium phlogopite), magnetite, Ni-rich sulfides, fayalite ($Fa_{>90}$), Ca-Fe-rich pyroxenes ($Fs_{10-50}Wo_{45-50}$) and andradite. Phyllosilicates replace primary Ca-rich minerals in chondrules and CAIs, which suggests mobilization of Ca during aqueous alteration. Magnetite nodules are replaced to various degrees by fayalite, Ca-Fe-rich pyroxenes and minor andradite. Fayalite veins crosscut fine-grained rims around chondrules and extend into the matrix. Thermodynamic analysis of the observed reactions indicates that they could have occurred at relatively low temperatures (<300 °C) in the presence of aqueous solutions. Oxygen isotopic compositions of the coexisting magnetite and fayalite plot close to the terrestrial fractionation line with large $\Delta^{18}O_{fayalite-magnetite}$ fractionation (~20‰). We infer that phyllosilicates, magnetite, fayalite, Ca-Fe-rich pyroxenes and andradite formed at relatively low temperatures (<300 °C) by fluid–rock interaction in an asteroidal environment.

Secondary fayalite and phyllosilicates are virtually absent in chondrules and CAIs in the $CV3_{oxA}$ lithology, which is present in Allende and its dark inclusions, Axtell, ALHA81258, ALH 84028, Lewis Cliff (LEW) 86006, and parts of the Mokoia and Vigarano breccias. Instead secondary nepheline, sodalite, and fayalitic olivine are common. Fayalitic olivine in chondrules replaces low-Ca pyroxenes and rims and veins forsterite grains; it also forms coarse lath-shaped grains in matrix. Secondary Ca-Fe-rich pyroxenes are abundant. We infer that the $CV3_{oxA}$ lithology experienced alteration at higher temperatures than the $CV3_{oxB}$ lithology. The presence of the reduced and $CV3_{oxA}$ lithologies in the Vigarano breccia and $CV3_{oxA}$ and $CV3_{oxB}$ lithologies in the Mokoia breccia indicates that all CV3 chondrites came from one heterogeneously altered asteroid. The metamorphosed clasts in Mokoia (Krot and Hutcheon, 1997) may be rare samples of the hotter interior of the CV asteroid. We conclude that the alteration features observed in the oxidized CV3 chondrites resulted from the fluid–rock interaction in an asteroid during progressive metamorphism of a heterogeneous mixture of ices and anhydrous materials mineralogically similar to the reduced CV3 chondrites.

INTRODUCTION

On the basis of the opaque mineralogy, McSween (1977) divided CV3 chondrites into the following subgroups: reduced, with Ni-poor metal and troilite, and oxidized, with magnetite, Ni- and Co-rich metal and Ni-rich sulfides (Table 1). Although there is a general agreement that the oxidized opaque assemblages resulted from the oxidation and sulfidization of the reduced opaque minerals, the time and place of this alteration (solar nebula or asteroidal body; before or after chondrule formation) remain uncertain (*e.g.*, McSween, 1977; Haggerty and McMahon, 1979; McMahon and Haggerty, 1980; Blum *et al.*, 1989; Rubin, 1991; Choi *et al.*, 1997).

In our review paper (Krot *et al.*, 1995), we showed that there are many other alteration features that are well developed in CAIs, chondrules and matrices in the oxidized subgroup and are rare or absent in the reduced subgroup. These features include: (1) fayalitic olivine rims around individual forsterite grains and forsterite phenocrysts in chondrules, (2) fayalitic olivine replacing low-Ca pyroxene grains in chondrules and matrices, (3) fayalitic olivine halos around relic inclusions of Ni-rich metal in forsterite, (4) lath-shaped fayalitic olivine (~Fa_{40-50}) in matrix (*e.g.*, Peck and Wood, 1987; Hua *et al.*, 1988; Weinbruch *et al.*, 1990, 1993; Krot *et al.*, 1997a; Hua and Buseck, 1997), (5) fayalite ($Fa_{>95}$) replacing opaque nodules in all major components in Kaba and Mokoia (Hua and Buseck, 1995; Krot *et al.*, 1997b), (6) grossular ($Ca_3Al_3Si_3O_{12}$), anorthite ($Ca_2Al_2Si_2O_8$), nepheline ($NaAlSiO_4$), sodalite ($Na_4[AlSiO_4]_3Cl$), wollastonite ($CaSiO_3$), salite–hedenbergite pyroxenes ($Fs_{10}Wo_{50}$-$Fs_{50}Wo_{50}$), andradite ($Ca_3Fe_2Si_3O_{12}$), and kirschsteinite ($CaFeSiO_4$) resulting from Fe–alkali–halogen metasomatism of chondrules and CAIs (*e.g.*, Hashimoto and Grossman, 1987; MacPherson *et al.*, 1988; McGuire and Hashimoto, 1989;

TABLE 1. List of CV3 chondrites studied.

Chondrite	Find/Fall	ss	Reference
Reduced subgroup			
Arch	find	S3	1
Efremovka	find	S4	1
Leoville	find	S3	1
Vigarano*	fall	S1–S2 br.	1,3
QUE 93429	find	S1	2
Oxidized subgroup			
Bali-like subgroup‡/lithology			
Bali	fall	S3	2
Grosnaja	fall	S3	2
Kaba	fall	S1	2,3,5
Mokoia†	fall	S1 br.	1–5
ALH 85006	find	S1	3
Allende-like subgroup‡/lithology			
Allende	fall	S1	1
Axtell	find	S1	6
ALHA81258	find	S1	3
ALH 84028	find	S1	2,3
LEW 86006	find	S1	3

ss = shock stage (Scott *et al.*, 1992; Krot et al., 1995).
*Breccia containing reduced and Allende-like lithologies (McSween, 1977; this study).
†Breccia containing Bali-like and Allende-like lithologies and heavily metamorphosed clasts (Cohen *et al.*, 1983; Krot and Hutcheon, 1997; this study). References: 1 = McSween (1977); 2 = Weisberg *et al.* (1997); 3 = Krot *et al.* (1997d); 4 = Cohen *et al.* (1983); 5 = Kimura and Ikeda (1997); 6 = Simon *et al.* (1994).
‡After Weisberg *et al.* (1997).

Ikeda and Kimura, 1995, 1996, 1997; Kimura and Ikeda, 1995, 1996, 1997), and (7) various phyllosilicates formed by aqueous alteration (*e.g.*, Keller and Buseck, 1989, 1990; Keller and McKay, 1993; Keller *et al.*, 1994; Tomeoka and Buseck, 1982a,b, 1990). Based on these observations, we concluded that the reduced CV3 chondrites are relatively primitive; whereas, all of the oxidized subgroup experienced alteration to various degrees.

There are two types of models, nebular and asteroidal, proposed for the explanation of the alteration features in the CV3 chondrites. According to the nebular models (*e.g.*, Palme and Wark, 1988; Rubin *et al.*, 1988; Palme and Fegley, 1990), evaporation of earlier condensed materials in regions with enhanced dust to gas ratios (up to 10^5 × solar) produced hot (~1700–1800 K) oxidized (H_2O/H_2 ratio ~ 1; cf. ~5×10^{-4} for solar gas) gas. Chondrules and CAIs in the oxidized CV3 chondrites were exposed to this gas resulting in their alteration; matrix condensed from this gas. In order to prevent intimate mixing of the altered (oxidized) and unaltered (reduced) materials, the alteration must have been followed by rapid accretion. Even if such a model could account for the alteration features observed in oxidized CV3 chondrites, a system with an atomic H/Si ratio of ~0.3 (dust to gas ratio is 10^5 × solar) hardly could be called nebular.

The first asteroidal model for alteration features in Allende was proposed by Housley and Cirlin (1983) and rejected by all other workers. Inspired by the aqueous alteration–dehydration model suggested by Kojima and Tomeoka (1994, 1996) for the Allende dark inclusion All-AF, Krot *et al.* (1995) inferred that CV3 chondrites of the oxidized subgroup experienced fluid-assisted metamorphism on the CV3 asteroid that resulted in most of the alteration features listed above.

Weisberg *et al.* (1997) proposed to divide oxidized CV3 chondrites into Bali-like ($CV3_{oxB}$) and Allende-like ($CV3_{oxA}$) subgroups (Table 1) on the basis of several criteria. Matrix olivine in the $CV3_{oxA}$ has a considerably more restricted compositional range than that in $CV3_{oxB}$; the $CV3_{oxA}$ subgroup has lower matrix abundances than the $CV3_{oxB}$ subgroup; phyllosilicates are less abundant, pure fayalite is absent, and bulk O isotopic compositions tend to be lighter than those of the $CV3_{oxB}$ subgroup (Weisberg *et al.*, 1997). The $CV3_{oxB}$ subgroup includes Bali, Kaba, parts of the Mokoia breccia, and possibly Grosnaja and ALH 85006; the latter two have not been characterized in detail yet and could be intermediate between $CV3_{oxB}$ and $CV3_{oxA}$. For example, matrix olivines in Grosnaja are compositionally similar to those in Allende (Scott *et al.*, 1988). Although we use this subdivision, we note that Bali itself contains heavily altered and relatively unaltered materials (Keller *et al.*, 1994), and neither portion may be representative of all the members of the Bali-like subgroup. For example, Kaba matrix contains pure fayalite and very fine-grained matrix olivines; whereas, our thin section of Bali has coarser lath-shaped matrix olivines and pure fayalite is absent.

Krot *et al.* (1997b,d) and Kimura and Ikeda (1997) showed that there are significant differences in the secondary minerals in chondrules in $CV3_{oxB}$ and $CV3_{oxA}$ subgroups. Secondary minerals in chondrules in $CV3_{oxB}$ meteorites (only chondrules in Kaba and Kaba-like portions of the Mokoia breccia have been studied) include phyllosilicates, magnetite, Ni-rich sulfides, fayalite, Ca-Fe-rich pyroxenes and andradite; secondary minerals observed in chondrules in all $CV3_{oxA}$ meteorites, including fayalitic olivine replacing low-Ca pyroxene and forsteritic olivine, and nepheline and sodalite replacing chondrule mesostasis, are absent.

The materials of the $CV3_{oxA}$ group are observed in Allende and its dark inclusions, ALHA81258, ALH 84028, LEW 86006, and parts of the Mokoia and Vigarano breccias. The secondary minerals in this subgroup include abundant nepheline, sodalite, kirschsteinite, wollastonite, Ca-Fe-rich pyroxenes, andradite, and several textural types of fayalitic olivine, including coarse-grained, lath-shaped matrix olivine, fayalitic olivine rims around forsterite grains and fayalitic olivine replacing low-Ca pyroxene grains. Fayalite ($Fa_{>90}$) is absent; phyllosilicates are very rare; Mokoia is the only exception (Tomeoka and Buseck, 1990; this study).

In this paper, we present new results on alteration minerals in chondrules and matrices in the $CV3_{oxB}$ and $CV3_{oxA}$ subgroups and update the Krot *et al.* (1995) model of the asteroidal alteration of CV3 chondrites in the light of these new results and recent work by Brearley and Prinz (1996), Brearley (1996, 1997a,b), and Tomeoka (1997). Our new results that are described in several abstracts (Krot *et al.*, 1996, 1997b,c,d) and will be discussed in more detail elsewhere (Krot *et al.*, 1998a,b) include: (1) differences in the secondary mineralization in the CV_{oxB} (Kaba and Kaba-like portions of the Mokoia breccia) and $CV3_{oxA}$ chondrules, (2) replacement of magnetite in the $CV3_{oxB}$ chondrules by fayalite and Ca-Fe-rich pyroxenes and *in situ* measurements of O isotopic compositions of the coexisting magnetite and fayalite, (3) thermodynamic analysis of the alteration reactions in the $CV3_{oxB}$ chondrules, and (4) phyllosilicate-bearing chondrule pseudomorphs in the Efremovka dark inclusions and their apparent I–Xe ages.

We infer that the reduced $CV3_{oxB}$ and $CV3_{oxA}$ subgroups may represent an alteration sequence within the CV3 asteroid and, hence, are lithological varieties of the CV3 asteroid. We argue that progressive alteration resulted from fluid–rock interaction in the CV3 asteroid that accreted as a heterogeneous mixture of ices and anhydrous materials mineralogically similar to the reduced CV3 chondrites Leoville and Efremovka and was subsequently heated during asteroidal thermal metamorphism.

ALTERATION MINERALS IN THE CV3 MATRICES

In this section, we discuss and compare textural and mineralogical characteristics of the matrices in the three subgroups of CV3 chondrites: reduced, $CV3_{oxB}$ and $CV3_{oxA}$. The key mineralogical features of the matrices in the three subgroups and in the primitive carbonaceous chondrite Acfer 094 (Greshake, 1997) are summarized in Table 2. The matrix mineralogy in the reduced subgroup in Table 2 is largely based on the transmission electron microscope (TEM) study of matrix in Leoville by Keller (1997) and Nakamura *et al.* (1992). In addition, we have observed the matrices in Leoville and Efremovka with the scanning electron microscope (SEM) (Fig. 1a,b); TEM study of the Efremovka matrix is lacking. The matrix mineralogy in the $CV3_{oxB}$ subgroup is based on our observations by SEM and electron microprobe analysis (EPMA) of matrices in Kaba, ALH 85006, Grosnaja, Bali, and Kaba-like parts of the Mokoia breccia, and TEM studies of matrices in Kaba, Bali, and Grosnaja by Keller and Buseck (1990), Zolensky (unpubl. data), Keller *et al.* (1994), and Keller and McKay (1993). The matrix mineralogy in the $CV3_{oxA}$ subgroup is based on our observations of matrices in Allende, Axtell, ALHA81258, LEW 86006, and Allende-like parts of the Mokoia breccia and observations described in Peck (1985), MacPherson *et al.* (1985), and Tomeoka and Buseck (1990). To emphasize the similarities in matrix mineralogies of the $CV3_{oxA}$ chondrites and Allende dark inclusions, we also list the latter in Table 2.

Leoville matrix is dominated by fine-grained (typically <1 μm) fayalitic olivine with a restricted compositional range between Fa_{50-60}; lath-shaped fayalitic olivine is not observed. Coarser-grained olivine varies in composition from Fa_{10-60}. Low-Ca pyroxenes are abundant; whereas high-Ca pyroxenes are rare and vary in composition from $Fs_{10}Wo_{50}$ to $Fs_{30}Wo_{50}$; hedenbergite is not observed. Feldspathoids and phyllosilicates are absent. Metal grains, <1 μm in size, are composed of kamacite (~5 atom% Ni) and taenite (40–55 atom% Ni). Irregularly shaped metal grains are surrounded by rims, up to 20 nm thick, of poorly graphitized C (PGC) (Keller, 1997). The reduced CV3 chondrites Leoville and Efremovka lack magnetite, tetrataenite, awaruite and pentlandite, which are observed in matrices of the oxidized CV3 chondrites.

Matrices in Kaba and Kaba-like portions of the Mokoia breccia consist of fine-grained fayalitic olivine, which commonly does not show lath-shaped morphology (Fig. 1c,d) and varies in composition from Fa_{20-40}; olivine fragments range in composition from Fa_{10-85} (Keller and Buseck, 1990). Large grains, up to 200 μm in size, of nearly pure fayalite are common (Fig. 1c,d). Although matrix in Bali is compacted by shock that complicates its mineralogical characterization (Scott *et al.*, 1992), it appears to consist of compositionally uniform fine-grained, lath-shaped fayalitic olivine; no pure fayalite grains were found in the thin section studied (Fig. 1f). Low-Ca pyroxenes are rare; whereas irregularly shaped Ca-Fe-rich pyroxene inclusions, 15–30 μm in diameter, are very abundant; some of them contain minor andradite and magnetite. These high-Ca pyroxenes are highly variable in composition ($Fs_{10}Wo_{50}$–$Fs_{50}Wo_{50}$) on a submicron scale (Fig. 2; Peck, 1985). Nepheline and sodalite are absent; whereas, saponite is very common (Keller and Buseck, 1990; this study). Metal is absent; magnetite occurs sparsely; Ni-rich sulfides are common.

Matrices in LEW 86006, ALHA81258, some portions of the Mokoia breccia, and Allende dark inclusions are texturally and mineralogically similar to that in Allende (Fig. 10.2.5 in Scott *et al.*, 1988; Fig. 1e,g–i). They consist predominantly of relatively coarse-grained, lath-shaped fayalitic olivines (5–10 μm) and fine-grained anhedral fayalitic olivines (<1 μm), which vary in composition from ~Fa_{40-50}; fayalite grains ($Fa_{>90}$) are absent. The grain size of lath-shaped fayalitic olivine varies significantly within the $CV3_{oxA}$ subgroup (Fig. 1g–i). Phyllosilicates are rare (Mokoia is the only exception, Tomeoka and Buseck, 1990; this study); whereas nepheline grains are common and typically enclose lath-shaped matrix olivines. There are abundant Ca-Fe-rich pyroxene inclusions, which are texturally and mineralogically similar to those in the $CV3_{oxB}$ matrices (Fig. 2; Peck, 1985); low-Ca pyroxene grains are absent. Nickel-rich metal and magnetite are scarce; Ni-rich sulfides are common.

Although there is little textural evidence in the CV3 matrices to distinguish primary and secondary anhydrous minerals, there are many clues from the chondrules and CAIs discussed below and from studies of matrices in primitive carbonaceous chondrites. On the basis of the grain size, the absence of phyllosilicates and magnetite, and the presence of metal and enstatite, Keller (1997) concluded that the Leoville matrix is very primitive compared to the matrices in the oxidized CV3 chondrites. The presence of abundant fayalitic olivine with restricted compositional ranges and the absence of amorphous material and matrix forsterites, which are common in the Acfer 094 matrix (Greshake, 1997), suggest that the Leoville matrix

TABLE 2. Matrix mineralogy in the CV3 chondrite subgroups, Allende dark inclusions and primitive carbonaceous chondrite Acfer 094.

	amorph. material	$Fo_{<2}$	low-Ca pyx	low-Ni metal	FeS	mgt*	pnt	$Fa_{>95}$‡	Ca-Fe-pyx§	phyl	neph	$Fa_{\sim 50}$†
Acfer 094	xx	xx	xx	–	xx	–	–	–	–	–	–	–
Reduced CV3s	–	–	xx	xx	xx	–	–	–	–	–	–	xx
Bali-like CV3s	–	–	–	–	–	x	xx	xx	xx	xx	–	xx
Allende-like CV3s	–	–	–	–	–	x	xx	–	xx	–	xx	xx
Allende dark incl.	–	–	–	–	–	x/–	xx	–	xx	–	x/–	xx

– = absent or rare, x = present, xx = common/abundant.
*Magnetite forms framboidal grains in the Bali-like matrices and massive nodules, probably from chondrules, in Bali-like and rarely in Allende-like matrices.
†Fine-grained (<1 μm) anhedral grains are common in all CV3 chondrites. Lath-shaped coarse grains (5–10 μm) are abundant in Allende-like matrix and are rare and smaller in Bali-like matrix.
‡Subhedral and euhedral grains up to 200 μm in size.
§Irregularly shaped salite–hedenbergite ± andradite ± magnetite inclusions 20–50 μm in size; also form veins in and rims around Allende dark inclusions.
Sources: Peck (1985), MacPherson *et al.* (1985), Keller *et al.* (1994), Keller and Buseck (1990), Tomeoka and Buseck (1990), Nakamura *et al.* (1992), Graham and Lee (1992), Greshake (1997), Weisberg *et al.* (1997), this study.
mgt = magnetite, pnt = pentlandite, phyl = phyllosilicates, neph = nepheline, pyx = pyroxene.

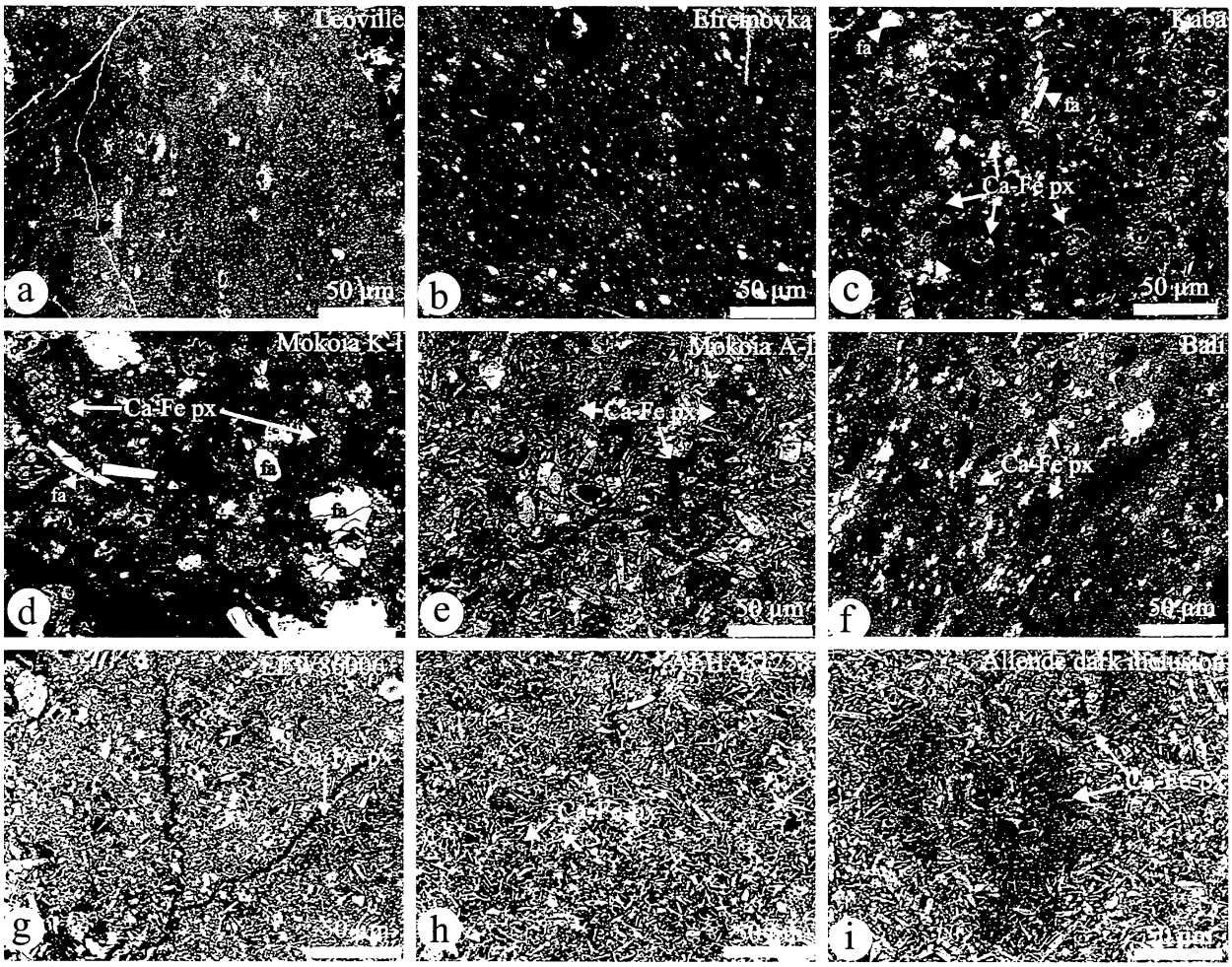

FIG. 1. Backscattered electron images of matrices that are representatives of the three types of subgroups/lithologies. (a,b) Reduced (Leoville, Efremovka), (c,d,f) Bali-like (Kaba, Kaba-like portion of the Mokoia breccia, Bali), and (e,g,h,i) Allende-like (Allende-like portion of Mokoia, LEW 86006, ALHA81258, Allende dark inclusion). (a,b) Matrices in Leoville and Efremovka consists of fine-grained (<1 μm) fayalitic olivines, abundant metal (white) and low-Ca pyroxene. Magnetite, phyllosilicates, Ca-Fe-rich pyroxenes and lath-shaped fayalitic olivine are absent. (c,d) Matrix in Kaba and a Kaba-like portion of Mokoia consists of fine-grained (<1 μm) fayalitic olivines, coarse subhedral and euhedral grains of nearly pure fayalite (fa, $Fa_{>90}$), abundant saponite and irregularly shaped Ca-Fe-rich pyroxene ± andradite inclusions (Ca-Fe px). The opaque minerals consist mainly of sulfides (white); metal is absent; magnetite is scarce. (f) Matrix in Bali is compacted during shock metamorphism. It appears to consist of lath-shaped fayalitic olivine that is coarser grained than matrix olivine in Kaba; fayalite grains are absent in the thin section studied. (e,g–i) Matrices in the Allende-like meteorites LEW 86006 and ALHA81258, an Allende-like portion of Mokoia and an Allende dark inclusion, consist of coarse (5–10 μm) lath-shaped and anhedral fine-grained (<1 μm) fayalitic olivines and abundant Ca-Fe-rich pyroxene inclusions ± andradite. The grain size of lath-shaped fayalitic olivine and the apparent diameters of the Ca-Fe-rich pyroxene inclusions increase from LEW 86006 to ALHA81258 to dark inclusion. Low-Ca pyroxenes and phyllosilicates are absent; nepheline grains are common and typically enclose lath-shaped matrix olivines. Nickel-rich metal and magnetite are scarce; Ni-rich sulfides are common.

could have experienced some alteration, nebular or asteroidal. The exact mechanism of fayalitic olivine growth in the Leoville matrix remains unclear; additional study is required. The absence of Ca-Fe-rich pyroxene ± andradite inclusions, fayalite, magnetite, Ni-rich metal and sulfides, phyllosilicates, nepheline and lath-shaped matrix olivines in the Leoville matrix, and their occurrence as alteration products in chondrules and CAIs in the oxidized CV3 chondrites and Allende dark inclusions (see Krot *et al.*, 1995; this study) suggest that these minerals in the matrices of the $CV3_{oxB}$ and $CV3_{oxA}$ subgroups of the oxidized CV3 chondrites also formed during alteration (Table 2).

ALTERATION MINERALS IN THE KABA-LIKE CHONDRULES

In this section, we describe our observations of alteration minerals in chondrules in Kaba (JSCK-1, -2, -3, USNM 1052-1) and in the Kaba-like portion in one Mokoia section (JSCM-1). Most Mokoia materials resemble Allende (Kimura and Ikeda, 1997; this study), but the section studied by Hua and Buseck (1995) appears to resemble Kaba. There are no published studies of the alteration minerals in chondrules in the Bali meteorite, except for the TEM studies of phyllosilicates (Keller and Buseck, 1990). Chondrules in Kaba and Kaba-like portions of Mokoia do not show any evidence for the Fe–alkali–halogen metasomatism that characterizes $CV3_{oxA}$ chondrules: fayalitic olivine rims around forsterite phenocrysts, replacement of low-Ca pyroxene by fayalitic olivine and chondrule mesostases by nepheline with minor sodalite, andradite, grossular, Ca-Fe-rich pyroxenes, and kirschsteinite (Krot *et al.*, 1997d).

Mineralogy and Petrography

Near the edges of chondrules, the anorthite-normative mesostasis ($\sim An_{90}Ab_{10}$) and low-Ca and high-Ca pyroxenes are extensively

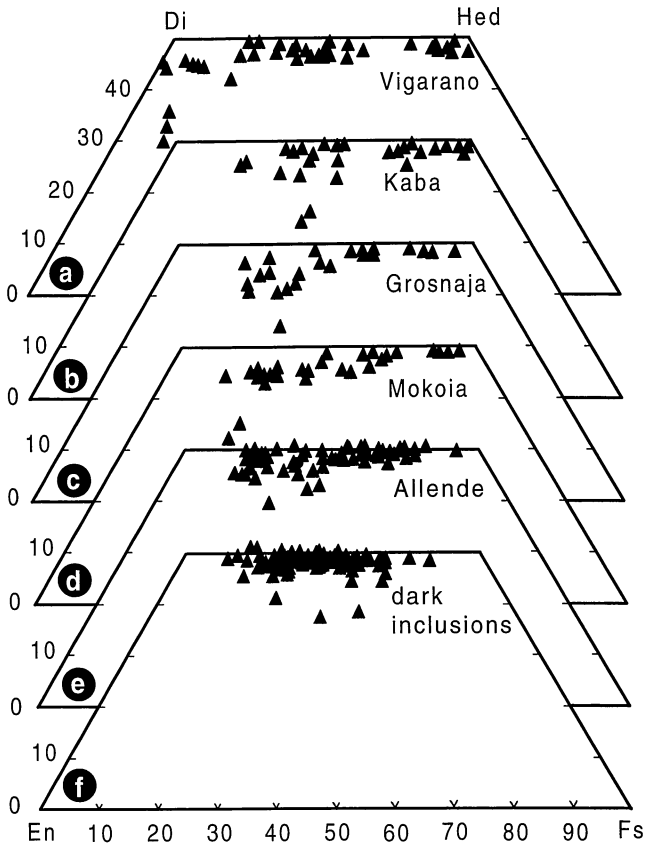

FIG. 2. Compositions of Ca-Fe-rich pyroxenes in matrices in the CV3 breccia Vigarano (a) and oxidized CV3 chondrites Kaba (b), Grosnaja (c), Mokoia (d) (Peck, 1985), Allende (e), and Allende dark inclusions (f) (this study). The Ca-Fe-rich pyroxenes in the Bali-like and Allende-like subgroups have similar compositions. The Ca-Fe-rich pyroxenes are virtually absent in the reduced CV3 chondrites Efremovka and Leoville but are very common in Vigarano, which suggests that it contains an oxidized CV3 component.

replaced by sodium phlogopite and saponite; chondrule cores contain glassy mesostasis (Fig. 3; Keller and Buseck, 1990). Both phyllosilicates are Ca-poor, which indicates nearly complete removal of Ca during aqueous alteration (Table 3). On the basis of compositional differences between primary anhydrous phases and phyllosilicates (Table 3) and x-ray imaging of the phyllosilicate-rich regions (Fig. 3b–d), we infer that Si, Al, Mg, Fe, Mn, and Na were redistributed during aqueous alteration as well.

Nearly all opaque nodules inside chondrules are replaced by magnetite (Figs. 3 and 4); relic Fe,Ni metal nodules are rare. Some of the relic Ni-rich metal grains inside forsterite phenocrysts are surrounded by fayalitic olivine halos, which are similar to those described in the Allende chondrules (Hua *et al.*, 1988; Weinbruch *et al.*, 1990). Magnetite nodules are replaced to various degrees by anhedral-to-euhedral fayalite grains ($Fa_{>95}$), porous Ca-Fe-rich pyroxenes, which vary in composition from Fs_5Wo_{50} and $Fs_{50}Wo_{50}$ on a submicron scale, and minor andradite (Figs. 4 and 5a,c,e). Secondary Ca-Fe-rich pyroxenes are texturally and compositionally different from massive, primary Ca-rich pyroxenes that occur as phenocrysts and crystallites in chondrule mesostasis (Fig. 5b,d). The composition and morphology of the fayalite grains are similar to those in the matrix described by Hua and Buseck (1995). The morphology of the fayalite grains appears to be correlated with the degree of the replacement of the magnetite nodules: anhedral fayalite grains are commonly observed in the incompletely replaced nodules; whereas subhedral and euhedral fayalite grains occur in the heavily altered nodules (Fig. 4a,b). It seems plausible that the morphology of the fayalite grains was controlled by the space available during their growth. Some of the fayalite grains are corroded by Ca-Fe-rich pyroxenes, which are texturally and compositionally similar to those replacing magnetite nodules (Fig. 4b). Fayalite and Ca-Fe-rich pyroxenes coexist with phyllosilicates; no evidence of corrosion of these anhydrous silicates by phyllosilicates was found (Fig. 4b).

Fayalite-bearing chondrules, like other chondrules, are typically surrounded by fine-grained rims that have distinct boundaries with matrix (Fig. 6a). Transmission electron microscope studies show that

TABLE 3. Representative electron microprobe analyses of primary and secondary minerals in chondrules in Kaba and Kaba-like portions of the Mokoia breccia.

	Primary			Secondary					
	pyx	fo	mes	mgt*	sap	Na-phl	hed	fa	andr
SiO_2	57.9	41.9	46.1	0.26	40.2	35.4	46.7	28.8	33.8
TiO_2	0.21	0.09	0.03	<0.02	0.05	0.04	0.06	<0.02	0.11
Al_2O_3	1.3	0.17	35.1	<0.02	9.1	24.8	<0.02	<0.02	0.09
Cr_2O_3	0.62	0.45	<0.02	1.5	0.66	0.04	<0.02	<0.02	0.06
FeO	0.61	0.79	0.44	87.3	3.2	4.2	27.4	70.2	34.2†
MnO	0.11	0.08	<0.02	0.04	0.03	0.12	0.34	0.27	<0.02
MgO	38.4	55.9	0.96	0.97	17.8	18.1	0.79	0.18	0.35
CaO	0.63	0.30	17.9	0.06	0.11	0.30	22.4	<0.02	31.6
Na_2O	n.a.	n.a.	1.2	<0.03	1.7	1.4	<0.03	<0.03	<0.03
K_2O	n.a.	n.a.	<0.02	<0.03	0.33	0.29	<0.03	<0.03	<0.03
total	99.8	99.7	101.7	90.5	73.2	84.7	97.7	99.4	100.2
Fa	–	0.8	–	–	–	–	–	99.3	–
Fs	1.2	–	–	–	–	–	47.6	–	–
Wo	0.9	–	–	–	–	–	49.9	–	–

n.a. = not analyzed.
*Contains 0.32 wt% NiO.
†As Fe_2O_3 in andradite.
pyx = low-Ca pyroxene; mes = mesostasis; mgt = magnetite; sap = saponite; Na-phl = Na-phlogopite; hed = hedenbergite; andr = andradite; fa = fayalite; fo = forsterite. For experimental procedures, see Krot *et al.* (1997a).

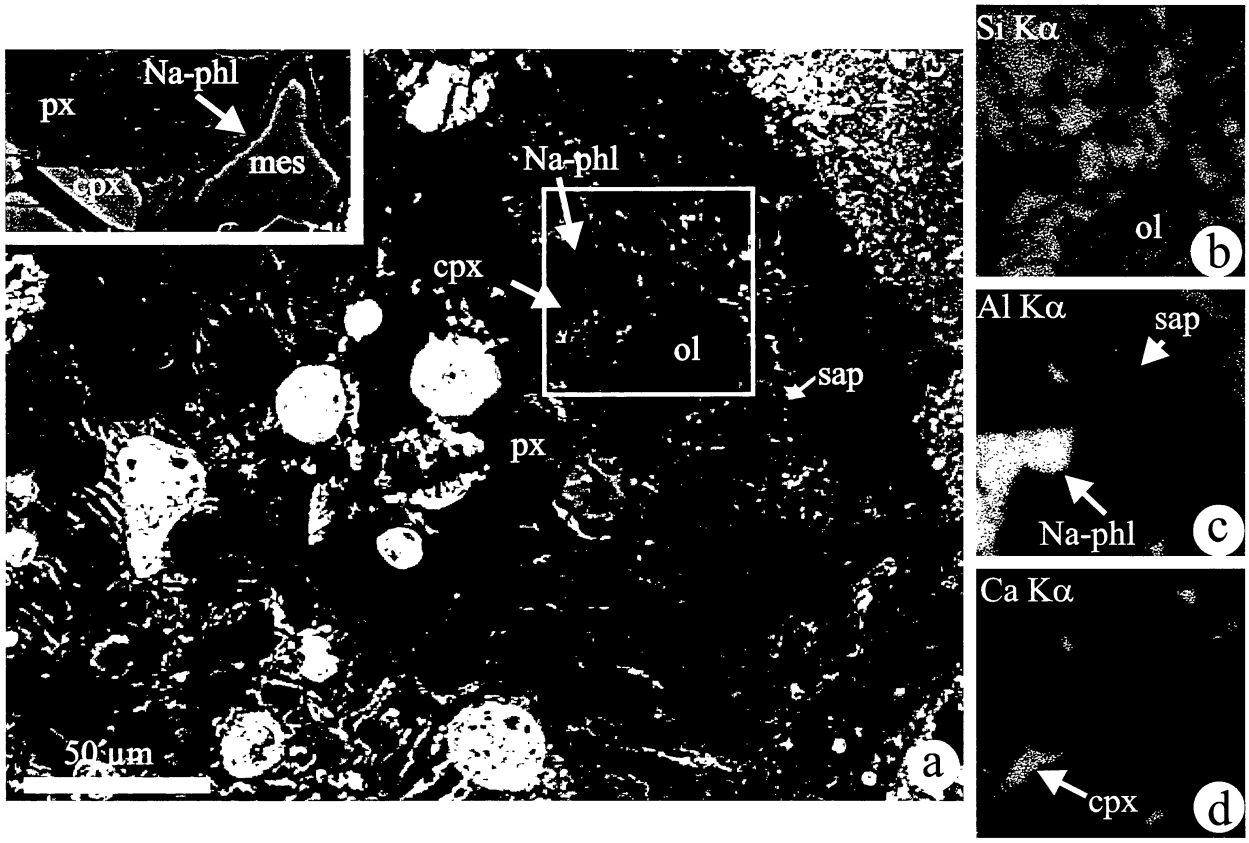

FIG. 3. Backscattered electron (a) and x-ray elemental maps in Si Kα (b), Al Kα (c) and Ca Kα (d) of a peripheral part of a porphyritic olivine–pyroxene chondrule in Kaba. Chondrule mesostasis and high-Ca pyroxenes (cpx) are replaced by sodium phlogopite (Na-phl); low-Ca pyroxene (px) grains are extensively corroded by saponite (sap). Low-Ca pyroxene grains are separated from saponite by thin layers of bronzitic pyroxene (light-gray) that is probably a by-product of alteration (Kimura and Ikeda, 1997). Both phyllosilicates are Ca-poor suggesting extensive mobilization of Ca during aqueous alteration. Inset in (a) shows a central portion of the chondrule. Anorthitic mesostasis is replaced by sodium phlogopite; low-Ca pyroxene is not altered.

these rims consist of saponite and abundant fine-grained (<1 μm) fayalitic olivines, which are texturally and compositionally similar to the matrix olivines (Krot *et al.*, 1997d). Clastic mineral fragments are virtually absent in the rims probably indicating that the rims are not clastic in origin. Anhedral fayalite–magnetite–sulfide grains are the only coarse-grained constituents in fine-grained rims. We infer that these fayalite grains are not fragments of larger fayalite grains; they grew *in situ* after rim compaction and did not have enough space to develop the euhedral morphology.

Fine-grained rims and a few chondrules are crosscut by fayalite–sulfide–magnetite veins, some of which extend into the matrix where they may connect with massive fayalite–magnetite–sulfide inclusions (Fig. 6b). In one forsteritic phenocryst, we found a fayalite vein that appears to fill a preexisting fracture (Fig. 6c). The compositional profiles across fayalite–forsterite boundaries and individual fayalite grains do not show any evidence of Fe–Mg exchange reactions, which suggests no reheating after fayalite formation.

Oxygen Isotopic Compositions of Magnetite and Fayalite

Oxygen isotopic compositions of the coexisting magnetite and fayalite grains in the fayalite-bearing chondrules in the Kaba-like lithology of the Mokoia breccia were analyzed *in situ* by the Cameca 1270 ion probe at UCLA. A defocused Cs^+ beam was used to sputter areas having diameters ~12 to 25 μm (Choi *et al.*, 1997). Negative $^{16}O^-$ ions were measured by a Faraday cup, and other isotopes were collected on an electron multiplier. The maximum OH-ion interference to the $^{17}O^-$signal was 0.5‰ but typically <0.1‰. The analyses plot close to the terrestrial fractionation line with large $\Delta^{18}O_{fayalite-magnetite}$ fractionation (~20‰) probably indicating low-temperature formation of magnetite and fayalite (Fig. 7). Because isotopic fractionation factors are small at high temperatures (Clayton, 1997), these results are inconsistent with a high-temperature nebular origin for fayalite that was proposed by Hua and Buseck (1995).

Thermodynamic Analysis of Alteration Reactions

The mineralogical and petrographic observations and O isotopic analyses of magnetite and fayalite described above indicate that the oxidation of metal to magnetite, replacement of anhydrous minerals by phyllosilicates, replacement of magnetite by fayalite, Ca-Fe-rich pyroxenes and andradite, and corrosion of fayalite by Ca-Fe-rich pyroxenes may have taken place at relatively low temperatures in the presence of aqueous solutions nearly simultaneously. In this section, we use thermodynamic analysis to check if the alteration features described above could have formed during an aqueous alteration responsible for the formation of phyllosilicates in CV3 chondrites. Since both the anhydrous minerals and phyllosilicates are equilibrated with the same aqueous solution, the mineral equilibria among these two mineral suites can be treated separately, if one knows the composition of the aqueous solution. In our calculations, we used activities of aqueous species calculated by Petaev and Mironenko (1997).

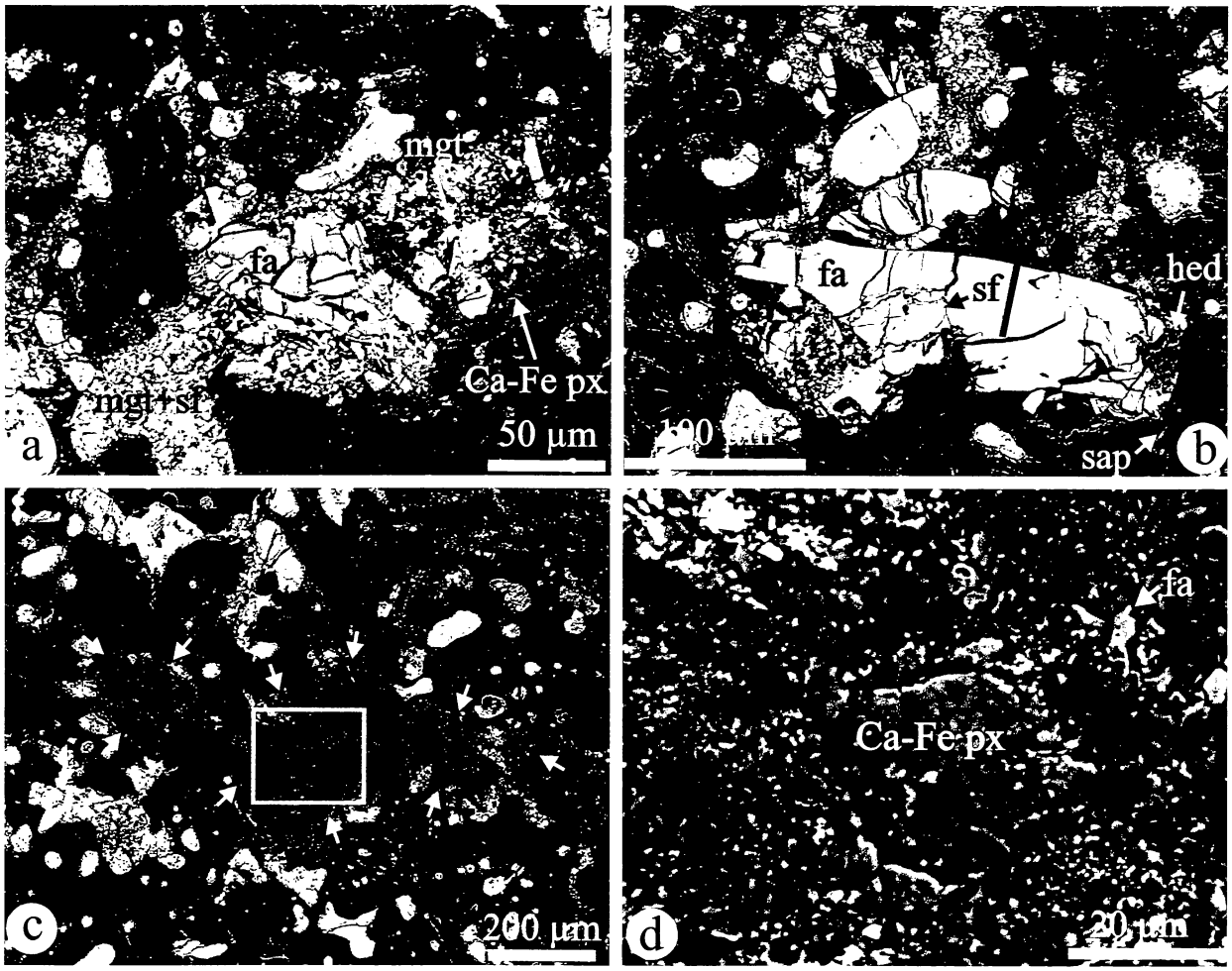

FIG. 4. Backscattered electron images of opaque nodules replaced to various degrees by fayalite ($Fa_{>90}$) and Ca-Fe-rich pyroxenes in Mg-rich chondrules in Kaba (a,c,d) and Kaba-like portions of the Mokoia breccia (b). (a) Magnetite–sulfide nodule (mgt + sf) incompletely replaced fayalite (fa) and Ca-Fe-rich pyroxenes (Ca–Fe px). Fayalite occurs as massive anhedral grains; anhedral inclusions of sulfides and magnetite are relict. (b) Opaque nodule completely replaced by subhedral and euhedral grains of fayalite. The largest fayalite grain is corroded by hedenbergite (hed), which is in direct contact with saponite (sap); the compositional profile across the fayalite (indicated by a black line) is flat. (c) Elongated opaque nodule with original boundary indicated by arrows is completely pseudomorphed by fine-grained mixtures of anhedral Ca-Fe-rich pyroxenes and minor fayalite. (d) Central region of opaque nodule in (c) showing large Ca-Fe-rich pyroxenes, which are compositionally variable, and micrometer-sized fayalite grains.

Thermodynamic modeling of aqueous alteration in a multisystem that consists of a reduced equivalent of CV3 chondrites (mg = 0.95) and variable amounts of H_2O (Petaev and Mironenko, 1997) shows that there are two distinct stages of the alteration process depending upon the water to rock ratio. At low water to rock ratios of <0.2–0.3, no aqueous solution is present in the system because all H_2O is consumed by the hydration and oxidation reactions. Hydrogen released by these reactions forms large volumes of gaseous phases that contain trace amounts of volatile anionic elements (H, O, S, Cl, and C). At this stage, an aqueous alteration would proceed as an isochemical process without appreciable redistribution of cationic elements. At higher water to rock ratios, an aqueous solution coexists with the altered rock and gaseous phase, and other elements (Na, Ca, Mg, Fe, Si and Al) can be redistributed as well. It is worthwhile to emphasize that the estimated water to rock ratios may reflect only local conditions in the region of alteration, in contrast to the water to rock ratio inferred from bulk O isotopic compositions of carbonaceous chondrites (Clayton and Mayeda, 1984; Clayton, 1997). The heterogeneous aqueous alteration of CV3 chondrites, inferred from the mineralogical observations (*e.g.*, Keller and Buseck, 1990; Tomeoka and Buseck, 1990; Keller *et al.*, 1994), is consistent with local variations in water to rock ratios within the CV3 asteroid.

According to the H_2O equation of state (*e.g.*, Naumov *et al.*, 1971), liquid water would coexist with the water vapor in the temperature range of 0.01–374.15 °C and the pressure range of ~0.006–225.65 bars, providing that the total pressure in the system is equal or higher than the pressure of saturated water steam at given temperature. At lower total pressures, all H_2O will be in a vapor phase. At temperatures >374.15 °C, an aqueous solution is unstable regardless of the total pressure. At lower temperatures, an upper temperature limit on aqueous solution stability is pressure-dependent. Because of their small sizes, the lithostatic pressures in asteroidal bodies are negligible, compared to those created by gases released during fluid–rock interaction and that fill the porous spaces (*e.g.*, Grimm and McSween, 1989). The upper limit of the pressure that the parent body can sustain depends upon the tensile strength of the rocks. Following the model of a carbonaceous chondrite parent body by Grimm and McSween (1989), we accept the value of the

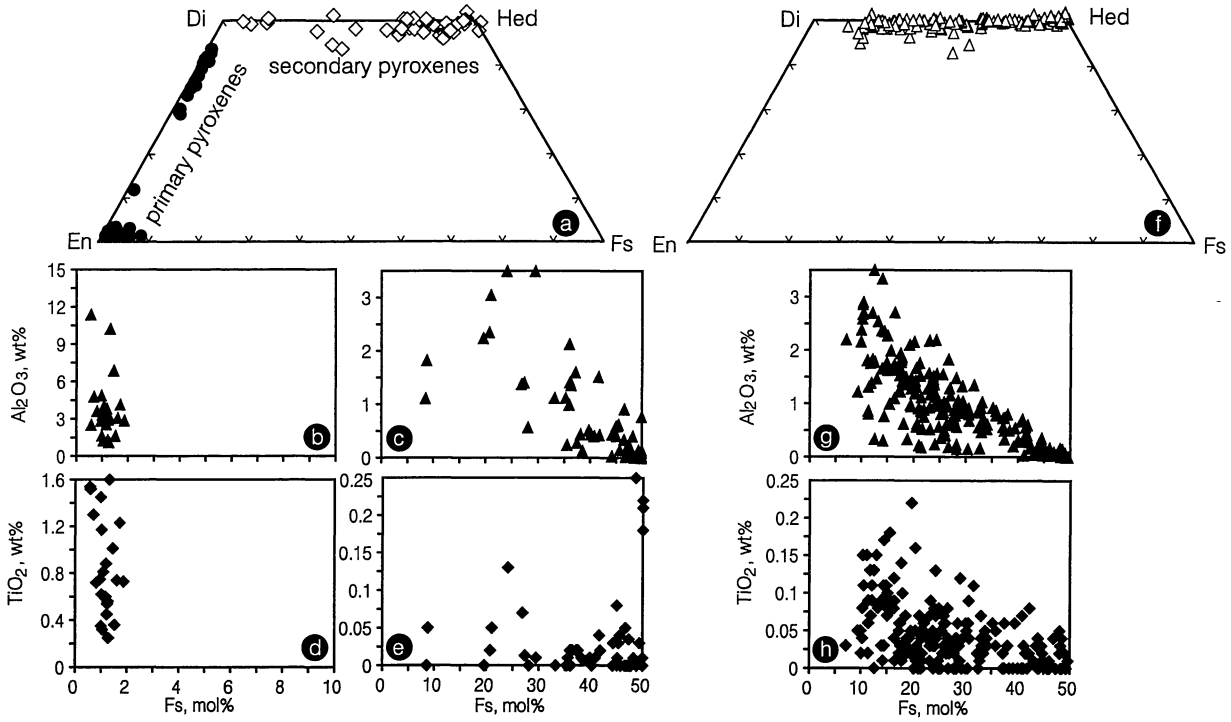

FIG. 5. Compositions of primary and secondary pyroxenes in the fayalite-bearing chondrules in Kaba and Kaba-like portions of the Mokoia breccia (a–e), and in veins in and rims around Allende dark inclusions (f–h). Note difference in vertical scales. All three textural types of the secondary Ca-Fe-rich pyroxenes are compositionally similar and absent in the reduced CV3 chondrites Efremovka and Leoville.

CV chondrite tensile strength of 100 bars. This places the upper temperature limit of ~310 °C on the presence of an aqueous solution on the CV chondrite parent body.

The alteration reactions supported by the petrographic observations are as follows:

$$3\ Fe_{(s)} + 4\ H_2O_{(g)} = Fe_3O_{4(s)} + 4\ H_{2(g)} \quad (1)$$

$$2\ Fe_{(s)} + SiO_{2(aq)} + 2\ H_2O_{(g)} = Fe_2SiO_{4(s)} + 2\ H_{2(g)} \quad (2)$$

$$2\ Fe_3O_{4(s)} + 3\ SiO_{2(aq)} + 2\ H_{2(g)} = 3\ Fe_2SiO_{4(s)} + 2\ H_2O_{(g)} \quad (3)$$

$$2\ Fe_3O_{4(s)} + 6\ SiO_{2(aq)} + 3\ Ca^{2+}_{(aq)} + 2\ H_{2(g)} = 3\ CaFeSi_2O_{6(s)} + 3\ Fe^{2+}_{(aq)} + 2\ H_2O_{(g)} \quad (4)$$

$$Fe_2SiO_{4(s)} + Ca^{2+}_{(aq)} + SiO_{2(aq)} = CaFeSi_2O_{6(s)} + Fe^{2+}_{(aq)} \quad (5)$$

$$9\ CaFeSi_2O_{6(s)} + 4\ H_2O_{(g)} = 3\ Ca_3Fe_2Si_3O_{12(s)} + Fe_3O_{4(s)} + 9\ SiO_{2(aq)} + 4\ H_{2(g)} \quad (6)$$

$$5\ Fe_2SiO_{4(s)} + 6\ Ca^{2+}_{(aq)} + SiO_{2(aq)} + 2\ H_2O_{(g)} = 2\ Ca_3Fe_2Si_3O_{12(s)} + 6\ Fe^{2+}_{(aq)} + 2\ H_{2(g)} \quad (7)$$

$$5\ Fe_3O_{4(s)} + 9\ SiO_{2(aq)} + 9\ Ca^{2+}_{(aq)} + 2\ H_{2(g)} = 3\ Ca_3Fe_2Si_3O_{12(s)} + 9\ Fe^{2+}_{(aq)} + 2\ H_2O_{(g)} \quad (8)$$

The corresponding equations linking the equilibrium constants of reactions (1–8) with the activities and partial pressures of components in aqueous and gaseous solutions are as follows:

$$\log K_1 = -4 \log [H_2O/H_2] \quad (9)$$

$$\log K_2 = -2 \log [H_2O/H_2] - \log [SiO_2] \quad (10)$$

$$\log K_3 = 2 \log [H_2O/H_2] - 3 \log [SiO_2] \quad (11)$$

$$\log K_4 = 2 \log [H_2O/H_2] + 3 \log [Fe^{2+}/Ca^{2+}] - 6 \log [SiO_2] \quad (12)$$

$$\log K_5 = \log [Fe^{2+}/Ca^{2+}] - \log [SiO_2] \quad (13)$$

$$\log K_6 = -4 \log [H_2O/H_2] + 9 \log [SiO_2] \quad (14)$$

$$\log K_7 = -2 \log [H_2O/H_2] + 6 \log [Fe^{2+}/Ca^{2+}] - \log [SiO_2] \quad (15)$$

$$\log K_8 = 2 \log [H_2O/H_2] + 9 \log [Fe^{2+}/Ca^{2+}] - 9 \log [SiO_2] \quad (16)$$

where K_i is the equilibrium constant of reaction (i); $[H_2O/H_2] = X_{H2O}/X_{H2}$; X_{H2O} and X_{H2} are the mixing ratios of H_2O and H_2 in the gaseous phase equilibrated with an aqueous solution; $P_{H2O} = X_{H2O} \times P_{tot}$ is the H_2O partial pressure in a gaseous phase; $P_{H2} = X_{H2} \times P_{tot}$ is the H_2 partial pressure in a gaseous phase; $[SiO_2]$, $[Ca^{2+}]$ and $[Fe^{2+}]$ are the activities of SiO_2, Ca^{2+}, and Fe^{2+} in an aqueous solution.

The calculations were done in the temperature range of 25–300 °C, at the total pressure of 100 bars and activities of SiO_2 in aqueous solution of 10^{-5} and 10^{-4}, which correspond to the activities of silica in the fluid equilibrated with the Kaba matrix at 100 bars and ~150 and ~210 °C, respectively (Petaev and Mironenko, 1997). All solid phases are treated as pure end-members of their solid solution series. In all cases, except for reaction (1), we assume that the gaseous phase, which is an ideal solution of H_2O vapor and H_2 gas, is in equilibrium with an aqueous solution. The results of the calculations are plotted in Fig. 8.

If water is supplied in a vapor phase only, then the initial $X_{H2O} = 1$, $P_{H2O} = P_{tot}$, and oxidation of metal to magnetite (reaction (1)) should proceed at any temperature (Fig. 8a). As reaction (1) proceeds, the continuous consumption of H_2O and release of H_2 gas decrease the X_{H2O} and $[H_2O/H_2]$ ratio in the gaseous phase. When the $[H_2O/H_2]$ reaches equilibrium value, the oxidation of metal ceases until either an H_2-rich gaseous phase is removed or a new portion of H_2O-rich vapor is supplied.

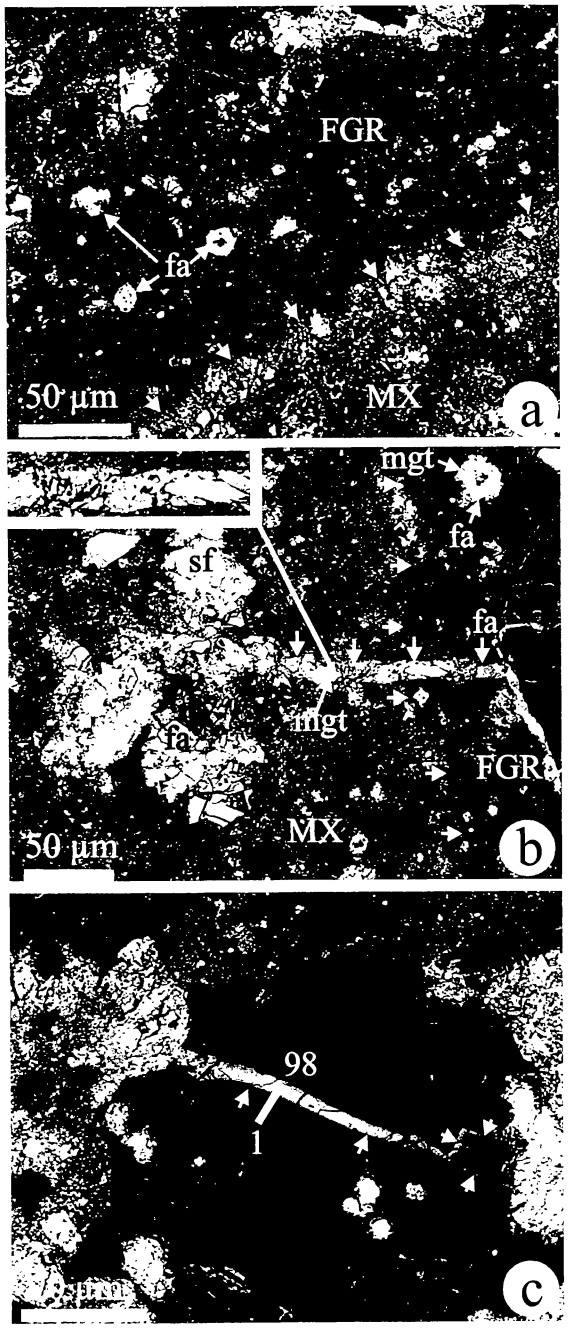

FIG. 6. Backscattered electron images of the fayalite-bearing veins and fine-grained rims in Kaba-like lithology of the Mokoia breccia (a,b) and Kaba (c). (a) The fine-grained rim (FGR) around the fayalite-bearing chondrule consists of abundant fine-grained fayalitic olivines and saponite; clastic mineral fragments are virtually absent. Anhedral fayalite–magnetite–sulfide grains (fa) are the only coarse-grained components. The boundary between fine-grained rim and matrix (MX) is distinct and indicated by arrows. (b) Porphyritic olivine–pyroxene chondrule (right) surrounded by fine-grained rim; the boundary between the rim and the matrix is indicated by arrows. Fayalite–magnetite–sulfide vein follows the boundary between the chondrule and fine-grained rim, crosscuts the rim and extends into the matrix where it connects with a massive fayalite–magnetite–sulfide inclusion. (c) Fayalite starts near a magnetite nodule and fills a fracture (indicated by arrows) in a forsteritic olivine phenocryst inside a porphyritic olivine–pyroxene chondrule. A compositional profile (indicated by white line) across a forsterite–fayalite boundary does not show any Fe–Mg diffusional exchange between the fayalite (Fa_{98}) and forsterite (Fa_1).

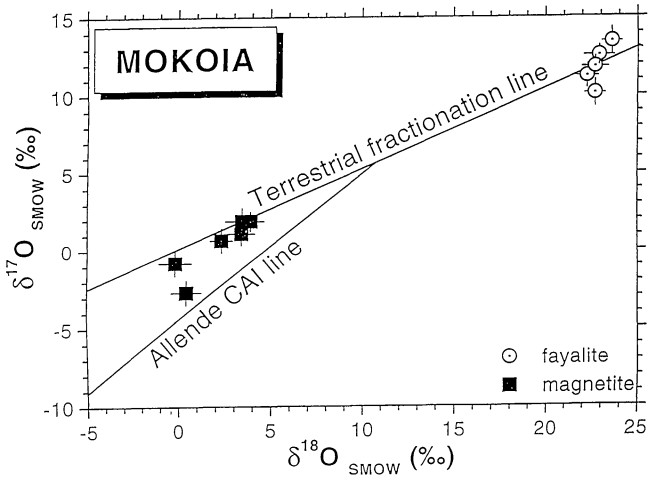

FIG. 7. Oxygen isotopic compositions of the coexisting magnetite and fayalite in the fayalite-bearing chondrules in Mokoia measured *in situ* by an ion-probe plot close to the terrestrial fractionation line with large $\Delta^{18}O_{fayalite-magnetite}$ fractionation (~20‰). Because isotopic fractionation factors are small at high temperatures (Clayton, 1997), these results are inconsistent with the high-temperature formation of fayalite in the solar nebula that Hua and Buseck (1995) proposed.

In the presence of liquid water or aqueous solution, the initial gaseous phase consists of pure water vapor (X_{H2O} = 1); the P_{H2O} (=P_{tot} = $P_{sat.steam}$) depends only on the temperature and X_{H2O} in an aqueous solution (Raoult law). As reaction (1) proceeds, the continuous release of H_2 into the gas increases the P_{tot} in the system and decreases the X_{H2O} and [H_2O/H_2] ratio in the gaseous phase. However, the liquid water will evaporate to maintain the P_{H2O} in the gaseous phase constant; as a result, the [H_2O/H_2] ratio in the gaseous phase in equilibrium with the aqueous solution (curve labeled 1 in Fig. 8a,b) will never reach the equilibrium value of reaction (1). This means that oxidation of metal to magnetite, release of H_2 gas and increase of total pressure will continue until P_{tot} exceeds tensile strength of the rock, which results in the rock fracturing and venting out the gaseous phase.

In the presence of aqueous silica ([SiO_2] = 10^{-5}), fayalite would directly replace metal (reaction (2)) and is stable at lower temperatures compared to magnetite (Fig. 8a). The increase of [SiO_2] values in the aqueous solution (10^{-4}) extends the fayalite stability field to higher temperatures (Fig. 8b). The [H_2O/H_2] ratio in the gaseous phase in equilibrium with aqueous solution (curve labeled 1 in Fig. 8a,b), which is higher than the equilibrium [H_2O/H_2] values for reaction (3) at temperatures ≳105–115 °C, diminishes the temperatures of the fayalite–magnetite phase boundary (*i.e.*, stabilizes magnetite). As a result, metal should be completely replaced by either magnetite or fayalite.

Figure 8c,d shows equilibrium phase relations between fayalite, magnetite, hedenbergite, and andradite *vs.* the Fe^{2+}/Ca^{2+} ratio in the aqueous solution with [SiO_2] values of 10^{-5} and 10^{-4}, respectively. The stability of hedenbergite and andradite depends on the Fe^{2+}/Ca^{2+} ratio in the aqueous solution; [SiO_2] has only minor effect. However, an increase in the [SiO_2] values significantly increases the temperature of the fayalite–magnetite transition. Fayalite and hedenbergite are low-temperature minerals; magnetite and andradite are stable at higher temperatures. Fayalite and andradite cannot coexist in equilibrium with one another suggesting that andradite cannot replace fayalite directly if equilibrium in the system is maintained. This conclusion is consistent with our mineralogical observations.

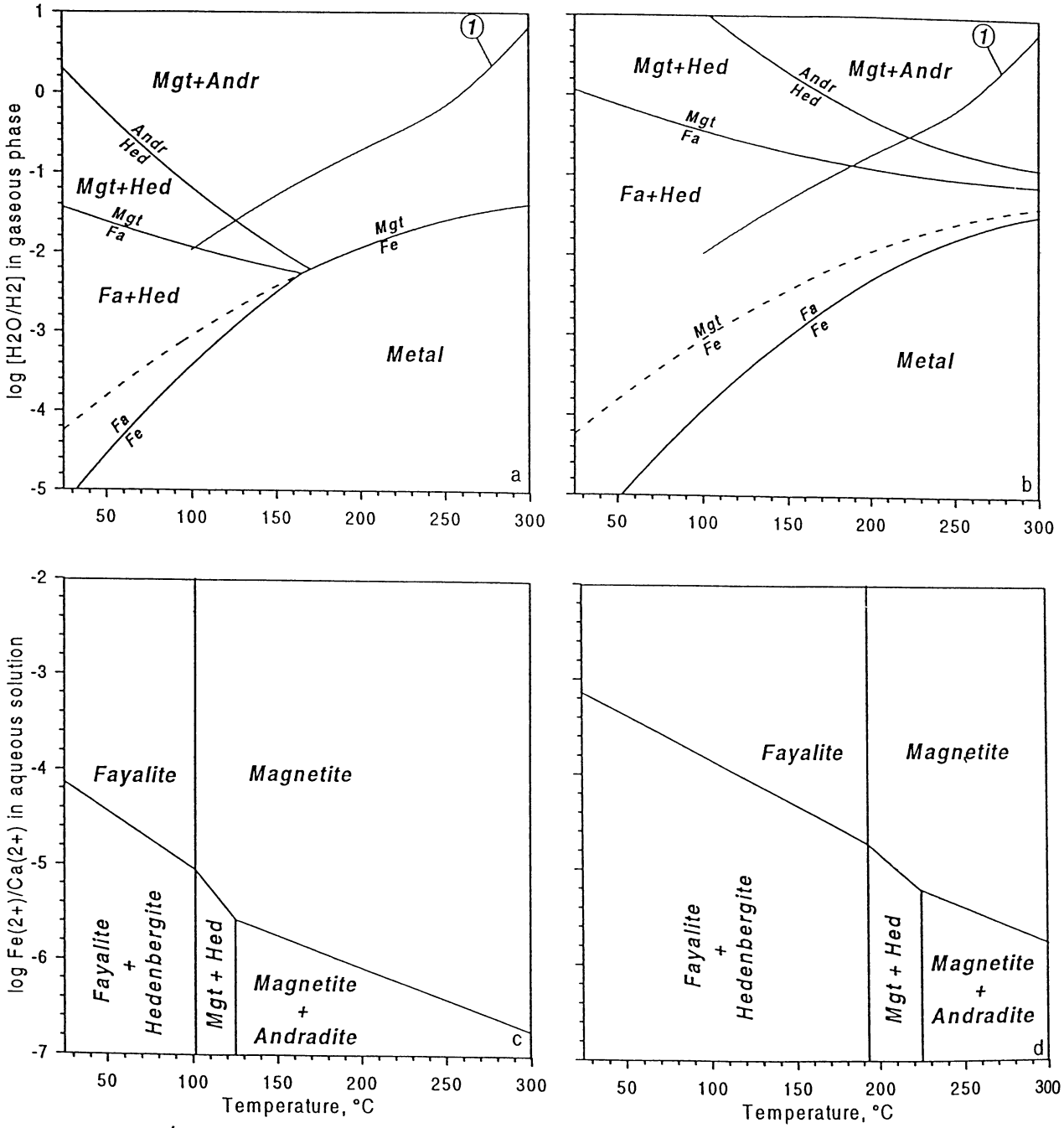

FIG. 8. Equilibrium phase relations in the Fe–Si–Ca–O–H system in the temperature range of 25–300 °C, at the total pressure 100 bars and activities of SiO_2 in aqueous solution 10^{-5} (a,c) and 10^{-4} (b,d). Curve labeled "1" represents the H_2O/H_2 ratio in the gaseous phase, which is in equilibrium with liquid water.

The thermodynamic analysis of the alteration reactions observed in the Kaba-like chondrules enhances the plausibility that magnetite, fayalite, hedenbergite, and andradite could have formed during relatively low-temperature aqueous alteration.

ALTERATION MINERALS IN THE ALLENDE-LIKE CHONDRULES AND ALLENDE DARK INCLUSIONS

The secondary minerals in the Allende-like chondrules and Allende dark inclusions include magnetite, Ni-rich metal and sulfides, fayalitic olivine, nepheline, sodalite, Ca-Fe-rich pyroxenes, andradite, wollastonite, kirschsteinite, and grossular; phyllosilicates are rare (Housley and Cirlin, 1983; Peck and Wood, 1987; Hua *et al.*, 1988; Weinbruch *et al.*, 1990; Kojima and Tomeoka, 1994, 1996; Ikeda and Kimura, 1995, 1996, 1997; Kimura and Ikeda, 1995, 1996, 1997; Krot *et al.*, 1995, 1997a; Brearley, 1997b). It seems likely, that most of these secondary minerals are genetically related (*e.g.*, Krot *et al.*, 1995; Ikeda and Kimura, 1995). In this section, we discuss new mineralogical and petrographic observations on the fayalitic olivine, nepheline, Ca-Fe-rich pyroxenes, andradite, wollastonite, and kirschsteinite that provide important constraints on

the progressive alteration of the CV3 chondrites (Krot *et al.*, 1997a–d, 1998a,b; Brearley, 1997a,b; Tomeoka, 1997). Our new mineralogical and petrographic observations include SEM, EPMA and TEM study of chondrule pseudomorphs in the Efremovka dark inclusions (Krot *et al.*, 1997c, 1998b) and $CV3_{oxA}$ chondrites, fayalitic olivine veins in the $CV3_{oxA}$ chondrites and Allende dark inclusions (Krot *et al.*, 1997a, this study), Ca-Fe-rich pyroxenes in the $CV3_{oxA}$ chondrules (this study), and Ca-rich veins and rims in the Allende dark inclusions (Krot *et al.*, 1996).

Fayalitic Olivine Halos, Rims, Pseudomorphs and Veins

Fayalite ($Fa_{>90}$) is absent in chondrules in the $CV3_{oxA}$ subgroup. Instead, fayalitic olivine ($Fa_{<50}$) is abundant (Krot *et al.*, 1997a; Weisberg and Prinz, 1997). There are several textural types of the fayalitic olivine: (1) halos around relic Ni-rich metal grains, (2) veins in and rims around forsterite grains, (3) olivine replacing low-Ca pyroxene and opaque nodules, and (4) veins crosscutting chondrules, fine-grained rims and matrices. The fayalitic olivine halos predate formation of other textural types of fayalitic olivine that probably formed contemporaneously with the lath-shaped fayalitic olivines in the matrices of the $CV3_{oxA}$ meteorites (Hua *et al.*, 1988; Palme and Fegley, 1990; Weinbruch *et al.*, 1990; Krot *et al.*, 1995, 1997a). This conclusion is consistent with the presence of fayalitic olivine halos in forsterite phenocrysts in the fayalite-bearing chondrules in the $CV3_{oxB}$ subgroup that lack all other textural types of fayalitic olivine (Krot *et al.*, 1997d). In this section, we focus on the origin of fayalitic olivine rims and fayalitic olivine replacing low-Ca pyroxene and olivine phenocrysts; fayalitic olivine halos will be discussed elsewhere.

The nebular scenario for the origin of fayalitic olivine in Allende involves high-temperature condensation from a hot (>1450 K) oxidizing nebular gas produced by evaporation of local nebular regions with high dust to gas ratios (*e.g.*, Hua *et al.*, 1988; Palme and Fegley, 1990; Weinbruch *et al.*, 1990; Dohmen *et al.*, 1997). However, this high-temperature condensation is inconsistent with the presence of pentlandite and PGC inclusions in the fayalitic olivines in Allende and its dark inclusions (Brearley and Prinz, 1996), and the presence of talc and biopyriboles in the Allende chondrules (Brearley, 1997b).

Thermodynamic analysis of high-temperature condensation of fayalitic olivine from the oxidized solar nebula by Palme and Fegley (1990) indicates that its condensation is possible only before condensation of any other Fe-bearing species, including Fe-metal, magnetite and sulfides. If Fe condenses as metal, which has the highest condensation temperature (~1450 K) among any other Fe-bearing species, and before condensation of fayalitic olivine, then the partial pressure of Fe in the gas decreases significantly and condensation of fayalitic olivine becomes impossible (see Figs. 5 and 6 in Palme and Fegley, 1990). Because sulfides (troilite, pyrrhotite, or pentlandite) condense at much lower temperatures (<700 K, Lauretta *et al.*, 1997) than fayalitic olivine (~1450 K), the presence of pentlandite inclusions in fayalitic olivine excludes its formation by high-temperature condensation.

Poorly graphitized C occurs as individual inclusions in fayalitic olivines in the Allende dark inclusions; it also forms thin films around other pentlandite, chromite and ilmenite inclusions in the fayalitic olivines (Brearley and Prinz, 1996). Because in the classical condensation sequence of the solar nebula gas, graphitic C does not become stable until temperatures have reached 600 K at 10^{-3} total pressure (Hayatsu *et al.*, 1980), Brearley and Prinz (1996) concluded that the presence of PGC inclusions in fayalitic olivine precludes its formation by high-temperature condensation.

Finally, Brearley (1997b) found that talc and biopyriboles that replace clinoenstatite in the Allende chondrules "invariably terminate at the interface with fayalitic olivine that also replaces clinoenstatite; they are never observed cutting across regions of fayalitic olivine. Where the partial replacement of the enstatite by fayalitic olivine has occurred, small inclusions of unreacted enstatite may be preserved. In some cases, these inclusions contain talc and disordered biopyriboles." Brearley (1997b) concluded that these observations strongly indicate that "the formation of fayalitic olivine occurred after, or perhaps contemporaneously with, the formation of the talc and biopyriboles." Because talc and biopyriboles cannot condense from a high-temperature nebular gas, even under extremely oxidizing conditions (Wood and Hashimoto, 1993), the origin of fayalitic olivine by high-temperature condensation is very unlikely.

Formation of fayalitic olivine during fluid-assisted metamorphism in the CV3 asteroid invokes different mechanisms, such as reaction between metal and low-Ca pyroxene in the presence of water vapor (Housley and Cirlin, 1983), and progressive aqueous alteration of matrix and chondrule silicates, followed by metamorphic dehydration (Krot *et al.*, 1995, 1997a). The mineralogical observations that support an asteroidal setting for the origin of fayalitic olivine include: (1) *in situ* replacement textures, including fayalitic olivine pseudomorphs after chondrules and mineral grains (Krot *et al.*, 1995, 1997a); (2) fayalitic olivine veins crosscutting chondrules and fine-grained rims and extending into the matrix (Kojima *et al.*, 1993; Krot *et al.*, 1997a; Tomeoka, 1997); and (3) hydrous phases replacing low-Ca pyroxene phenocrysts and possibly predating formation of fayalitic olivine in the Allende chondrules (Brearley, 1997a).

Many chondrules in the Allende dark inclusions are nearly completely pseudomorphed by fayalitic olivines (Fa_{40-50}) resulting in the formation of chondrule-like objects composed of porous or closely packed, lath-shaped fayalitic olivine and rare relic grains of aluminum diopside (Kojima and Tomeoka, 1994; Krot *et al.*, 1995, 1997a). Because the chondrule textures of most of these objects are poorly preserved and the fayalitic olivines are texturally and compositionally similar to the matrix olivines, some researchers argued that they are not chondrules but aggregates of nebular condensates (*e.g.*, Palme *et al.*, 1989; Kurat *et al.*, 1989; Weisberg and Prinz, 1997). However, this argument is invalidated by the discovery of partly replaced chondrules with preserved relic forsteritic olivine cores, both in the Allende dark inclusions (Fig. 7 in Krot *et al.*, 1997a) and in the $CV3_{oxA}$ chondrites (Fig. 9a). In these pseudomorphs, the relic forsterite grains are surrounded by fayalitic olivine rims, which are texturally and compositionally similar to those in the Allende, suggesting that these rims formed by the replacement of the forsterites and not by condensation. In addition, there is strong textural evidence for *in situ* replacement of forsterite phenocrysts in chondrules (Fig. 7 in Krot *et al.*, 1997a) and isolated olivine grains by fayalitic olivine (Fig. 9b).

Additional arguments favoring a replacement origin of the fayalitic olivine in Allende come from the Efremovka dark inclusions containing complete and incomplete chondrule pseudomorphs with very well-preserved chondrule textures (Fig. 9c,d). Relic forsteritic phenocrysts in the incomplete pseudomorphs are replaced and veined by abundant fayalitic olivine and minor phyllosilicates (Krot *et al.*, 1997c, 1998b). The fayalitic olivines are compositionally

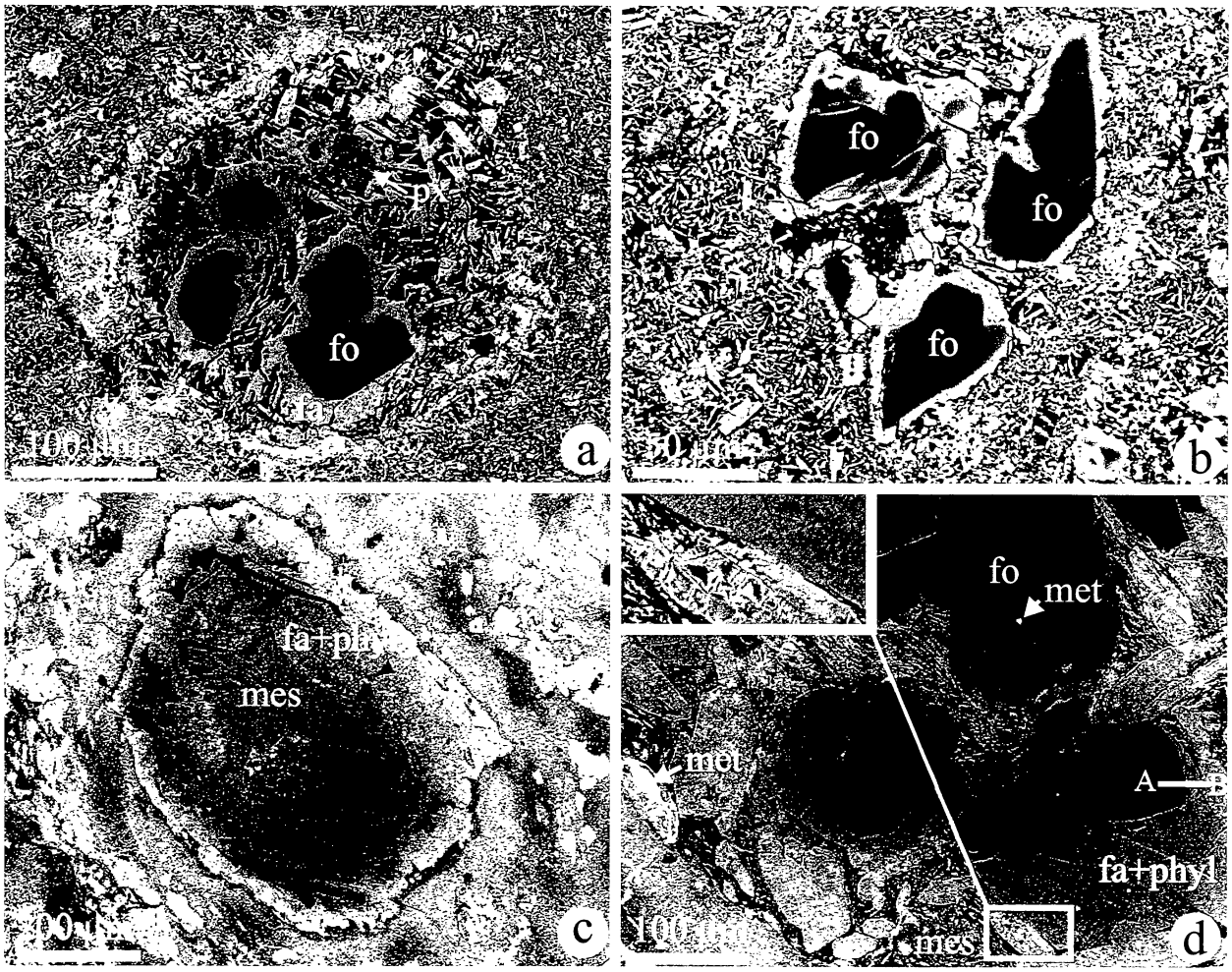

FIG. 9. Backscattered electron images of fayalitic olivine in the oxidized CV3 chondrite ALHA81258 (a), Allende dark inclusion (b), and Efremovka dark inclusion (c,d). (a) Type I porphyritic chondrule with low-Ca pyroxene phenocrysts incompletely pseudomorphed by fayalitic olivine; some of the olivines have lath-shaped morphology. Three relict olivine phenocrysts have fayalitic olivine rims. Relict low-Ca pyroxenes (px) are preserved between fayalitic olivine laths. (b) Fayalitic olivine (fa) rims (marked by arrows), which are texturally and compositionally similar to those in the Allende host, surround three parts of a single forsterite (fo) grain (all parts are in optical continuity) indicating that these rims formed by *in situ* alteration of a single forsterite grain, not by condensation. (c) Porphyritic chondrule completely pseudomorphed by fine-grained fayalitic olivine and phyllosilicates. The chondrule texture is well preserved. (d) Porphyritic olivine–pyroxene chondrule incompletely pseudomorphed by fine-grained fayalitic olivine and minor phyllosilicates (fa + phyl). Some altered phenocrysts show characteristic serpentinite texture (see inside white box). The compositional profiles across forsterite–fayalite boundaries are steep and similar to those described in Allende (*e.g.*, Hua *et al.*, 1988; Weinbruch *et al.*, 1990). Low-Ni metal is preserved only inside forsterite grains (center); the altered metal grains (left) are Ni- and Co-rich. px = low-Ca pyroxene, mes = mesostasis, met = metal.

similar to those in Allende but are finer grained and only occasionally show lath-shaped morphology. The compositional profiles across fayalitic olivine–forsterite boundaries are steep and reminiscent of those of Allende.

Fayalitic olivine-sulfide veins crosscut fine-grained rims, chondrules and extend into the matrix in Allende, ALH 84028, Allende-like parts of the Mokoia breccia, Allende and Vigarano dark inclusions (*e.g.*, Kojima *et al.*, 1993; Kojima and Tomeoka, 1996; Tomeoka, 1997; Krot *et al.*, 1997a,d; this study). The fayalitic olivine veins in ALH 84028, Allende and its dark inclusions (Fig. 12a) are compositionally similar to the matrix olivines ($Fa_{\sim 50}$); those in Mokoia show inverse (core-to-rim) compositional zoning from Fa_{80} to Fa_{40}. Because veins crosscutting several chondritic components postdate agglomeration and lithification of these components into bodies of various sizes, this process must be asteroidal.

Many Allende chondrules contain minor calcic amphiboles, disordered biopyriboles and talc replacing low-Ca pyroxene phenocrysts (Brearley, 1997a). These hydrous phases either predate formation of fayalitic olivine replacing low-Ca pyroxene in the same chondrules or they formed contemporaneously with fayalitic olivine. Because the kinetics of hydration reactions of the crystalline phases in the solar nebula gas are extremely slow, much longer than the lifetime of the solar nebula, it is generally accepted that hydrous silicates could have formed by reactions between liquid or gaseous water and anhydrous silicates only in an asteroidal environment (*e.g.*, Fegley, 1997). This implies that fayalitic olivine in the Allende chondrules formed in the CV3 asteroid rather than in the solar nebula.

Krot *et al.* (1997a) hypothesized that lath-shaped matrix olivine and fayalitic olivine rims around forsterites formed by progressive aqueous alteration and subsequent dehydration of the phyllosilicates. Supporting evidence is provided by the microstructures of matrix olivine, which are similar to those described in dehydrated phyllosilicates in CM chondrites (Akai, 1988), and include voids, inclusions of pentlandite and PGC (Krot *et al.*, 1997a; Brearley and

Prinz, 1996; Brearley, 1996, 1997b; Zolensky and Krot, 1996), the observed relic phyllosilicates associated with fayalitic olivine in chondrules in the Efremovka dark inclusions (Krot *et al.*, 1997c, 1998b) and hydrous silicates in the Allende chondrules (Brearley, 1997a). The origin of lath-shaped fayalitic olivine by dehydration of phyllosilicates appears to be inconsistent with the presence of saponite replacing lath-shaped matrix olivine in Bali and the Mokoia breccia (Keller *et al.*, 1994; Tomeoka and Buseck, 1990; this study). We infer that these meteorites may have experienced retrograde metamorphism or multistage aqueous alteration.

The exact mechanism of the fayalitic olivine growth remains unknown, and it is possible that the precursor phase was not phyllosilicate but olivine that was partly altered to phyllosilicates or poorly ordered phases on a submicron scale. In this case, the degree of hydration could have been comparable with estimates by Clayton *et al.* (1997). Metamorphic reactions in the presence of aqueous solutions also must have played an important role in the formation of fayalitic olivine from low-Ca pyroxene (Housley and Cirlin, 1983; Brearley, 1997b). On the basis of the presence of disordered biopyriboles and talc in Allende chondrules, Brearley (1997a) concluded that the peak metamorphic temperatures experienced by Allende did not exceed 340 °C, which is 150–200 °C lower than other independent estimates (see Krot *et al.*, 1995).

Some of the opaque nodules in the fayalitic olivine-bearing chondrules in the $CV3_{oxA}$ subgroup are replaced by Ca-Fe-rich pyroxenes that are texturally and compositionally similar to those in the Kaba-like chondrules (Figs. 4 and 10). In the $CV3_{oxA}$ chondrules, these Ca-Fe-rich pyroxenes are surrounded by fayalitic olivine replacing low-Ca pyroxene phenocrysts (Fig. 10b,e,f); they are also observed in chondrule cores that lack fayalitic olivines (Fig. 10c,d). In the Kaba-like chondrules, the Ca-Fe-rich pyroxenes are surrounded by enstatite and forsterite, which show no evidence of replacement by fayalitic olivine (Fig. 4). This suggests that fayalitic olivine, which is abundant in the $CV3_{oxA}$ chondrules and absent in the Kaba-like chondrules, may have formed after or contemporaneously with Ca-Fe-rich pyroxenes replacing opaque nodules.

Formation of Nepheline and Sodalite, and Mobilization of Sodium

Nepheline and sodalite replace melilite in CAIs and they both corrode the plagioclase-normative mesostasis in chondrules; nepheline is also associated with matrix olivines in the $CV3_{oxA}$ subgroup (Krot *et al.*, 1995, 1997a). Ikeda and Kimura (1997) concluded that these minerals formed at relatively low temperatures (<800 K) by gas–solid reactions in the solar nebula (*e.g.*, Ikeda and Kimura, 1995, 1996, 1997). The presence of nepheline grains enclosing lath-shaped matrix olivines, and intergrowths of nepheline and fayalitic olivine replacing isolated forsterite grains in Allende dark inclusions, indicate that nepheline either postdates formation of these textural types of fayalitic olivine or both minerals formed contemporaneously (Krot *et al.*, 1997a).

Palme *et al.* (1988) showed that despite the heterogeneous distribution of Na in CV3 chondrites, the oxidized chondrites have significantly higher bulk Na contents than the reduced chondrites. Although most of the Allende dark inclusions are mineralogically and chemically similar to the host Allende, their bulk Na contents are typically lower than in the reduced CV3 chondrites (Bischoff *et al.*, 1988). Plagioclase-normative chondrule mesostases, nepheline, sodalite, and phyllosilicates are the major mineral carriers of Na in CV3 chondrites. Nepheline, sodalite, saponite and sodium phlogopite are common secondary minerals in the oxidized subgroup of the CV3 chondrites but virtually absent in the reduced CV3 chondrites Efremovka and Leoville (Keller, 1997; this study). Because unaltered mesostases in the reduced and oxidized subgroups are compositionally identical (Krot, unpubl. data), we infer that the differences in bulk Na contents between these subgroups are mainly due to the secondary alteration.

All four analyzed oxidized CV3 chondrites, including anhydrous Allende and aqueously altered Bali, Grosnaja, and Mokoia (Keller *et al.*, 1994; Keller and McKay, 1993; Tomeoka and Buseck, 1990), have relatively similar bulk Na contents (Fig. 2 in Krot *et al.*, 1995). Although the bulk Na content of Kaba is not known, there is no reason to believe that it should be different from those of Bali, Grosnaja and Mokoia, which all show similar alteration features (*e.g.*, Krot *et al.*, 1997d; Weisberg *et al.*, 1997; this study). Nepheline and sodalite, which are the major Na-bearing secondary minerals in anhydrous Allende, are virtually absent in Kaba, which contains abundant sodium phlogopite and saponite. These differences may have resulted from higher temperature alteration of the Allende-like meteorites.

The presence of nepheline-bearing veins crosscutting Allende dark inclusions (Tomeoka, 1997) and the observed depletion in bulk Na contents in most of the Allende dark inclusions (Bischoff *et al.*, 1988) supports mobilization of Na during fluid-assisted metamorphism. Because most of the Allende dark inclusions are depleted in Na (All-AF is enriched in Na, Palme *et al.*, 1989), it seems plausible that Na lost from them was redistributed into the $CV3_{oxA}$ and $CV3_{oxB}$ subgroups of the oxidized CV3 chondrites.

Late-Stage Formation of Calcium-Iron-rich Pyroxenes, Andradite, Wollastonite, and Kirschsteinite

The alkali metasomatic alteration of chondrules and CAIs in Allende resulted in Ca loss from the primary minerals (melilite and anorthitic mesostasis) and crystallization of the secondary Ca-rich minerals, including grossular, anorthite, wollastonite, Ca-Fe-rich pyroxenes, andradite, and kirschsteinite, in veins in and rims around CAIs and in mesostases in chondrules (*e.g.*, Allen *et al.*, 1978; Hashimoto and Grossman, 1987; MacPherson *et al.*, 1981; McGuire and Hashimoto, 1989; Ikeda and Kimura, 1995, 1996, 1997; Kimura and Ikeda, 1995, 1996, 1997). The Ca-Fe-rich pyroxenes vary in composition from diopside to hedenbergite; wollastonite occasionally forms needle-shaped crystals. These secondary minerals have been attributed to the metasomatic alteration of CAIs and chondrules in the nebula (*e.g.*, Ikeda and Kimura, 1997) or to accretion of nebular condensates (MacPherson *et al.*, 1985). In this section, we discuss similar mineral assemblages in the Ca-rich veins in and rims around the Allende dark inclusions, which we suggest favor asteroidal formation of these secondary phases (Krot *et al.*, 1996, 1997b, 1998a).

Some of the Allende dark inclusions are crosscut by Ca-rich veins that may extend to the boundaries with the host Allende and form multilayered rims around them (Fig. 11a–c). The Ca-rich veins consist of Ca-Fe-rich pyroxenes and minor andradite; they crosscut matrices composed of lath-shaped fayalitic olivine and replace fayalitic olivine rims around forsterite grains (Fig. 11d,e). The exterior portions of the rimmed dark inclusions show depletion in Ca (Fig. 11b). The Ca-rich rims are composed of Ca-Fe-rich pyroxenes, andradite, wollastonite and minor kirschsteinite; wollastonite occasionally forms needle-shaped crystals (Krot *et al.*, 1996). The Ca-Fe-rich pyroxenes in veins and rims are texturally and compositionally (Fig. 5b) similar to those in rims around CAIs (Fig. 8 in

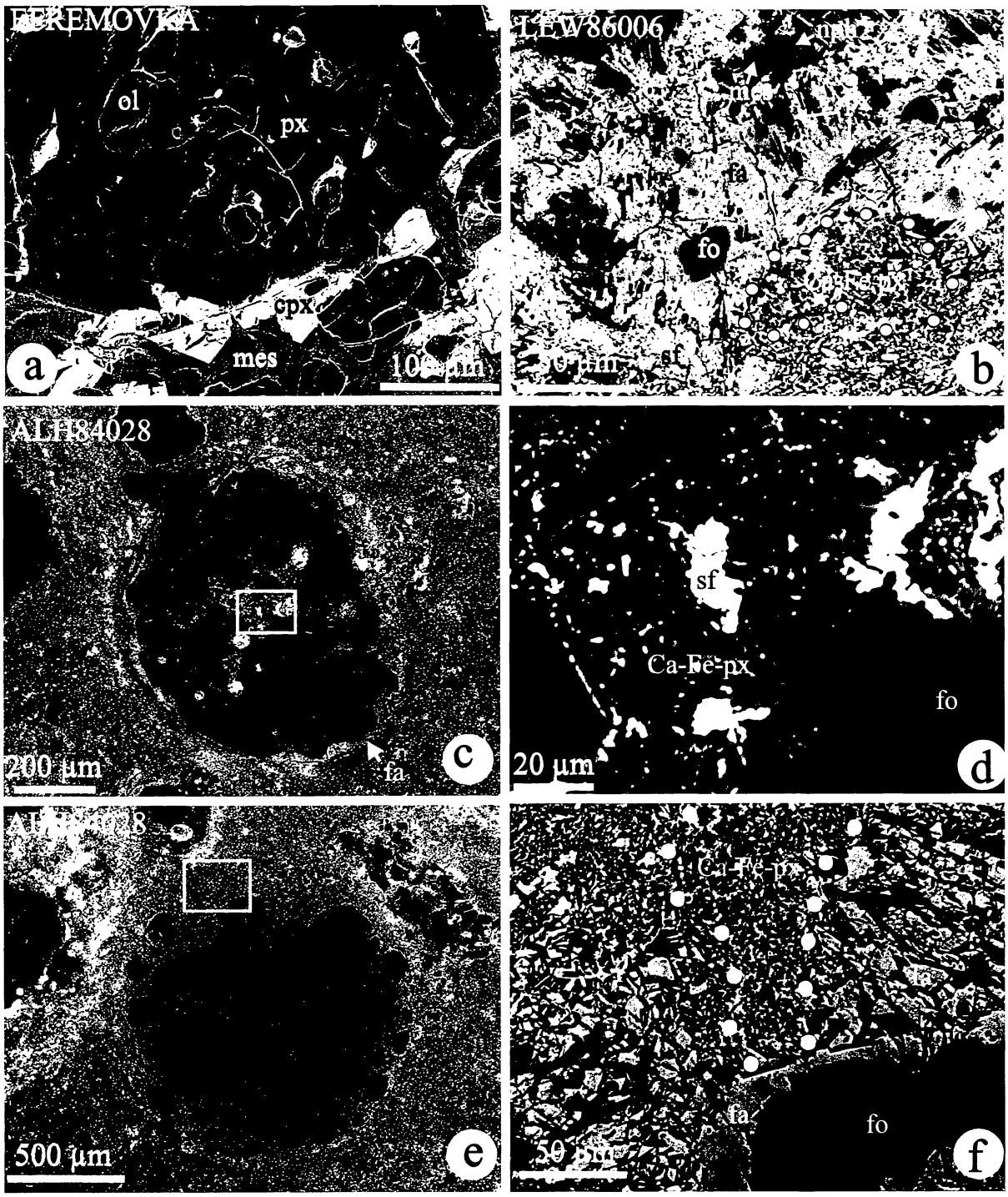

FIG. 10. Backscattered electron images showing alteration of porphyritic chondrules in CV3 chondrites: unaltered chondrule in the reduced CV3 chondrite Efremovka (a); and altered chondrules in the oxidized CV3 chondrites LEW 86006 (b) and ALH 84028 (c–f). (a) Low-Ca pyroxene grain (px) with poikilitic inclusions of forsteritic olivines (ol) is overgrown by Al-diopsidic pyroxenes (cpx) embedded in glassy mesostasis (mes). None of the minerals are altered. (b) Low-Ca pyroxene (px) is almost entirely replaced by fayalitic olivine (fa); forsterite grains, poikilitically enclosed in the pyroxenes, are relict. Anorthitic mesostasis is partly replaced by nepheline (nph). An opaque nodule (outlined by black dots), partly surrounded by fayalitic olivine, is replaced by Ca-Fe-rich pyroxenes (Ca–Fe px). The opaque phases consist mainly of Ni-rich sulfides (sf); magnetite is absent. (c,d) Ca-Fe-rich pyroxenes replace an opaque nodule in the central part of a porhyritic olivine chondrule; sulfide grains (sf) are relict; forsterite grains do not show evidence of alteration. Forsterite grains in the peripheral part of the chondrule are surrounded by thick fayalitic olivine rims. (e,f) Porphyritic olivine–pyroxene chondrule with low-Ca pyroxene grains preferentially replaced by fayalitic olivine; forsterite grains are surrounded by fayalitic olivine rims. Porous and compositionally variable Ca-Fe-rich pyroxenes occur in the replaced outer portion of the chondrule where they occupy a rounded region (outlined by dots) between fayalitic olivines. We infer that these pyroxenes formed by replacement of an opaque nodule.

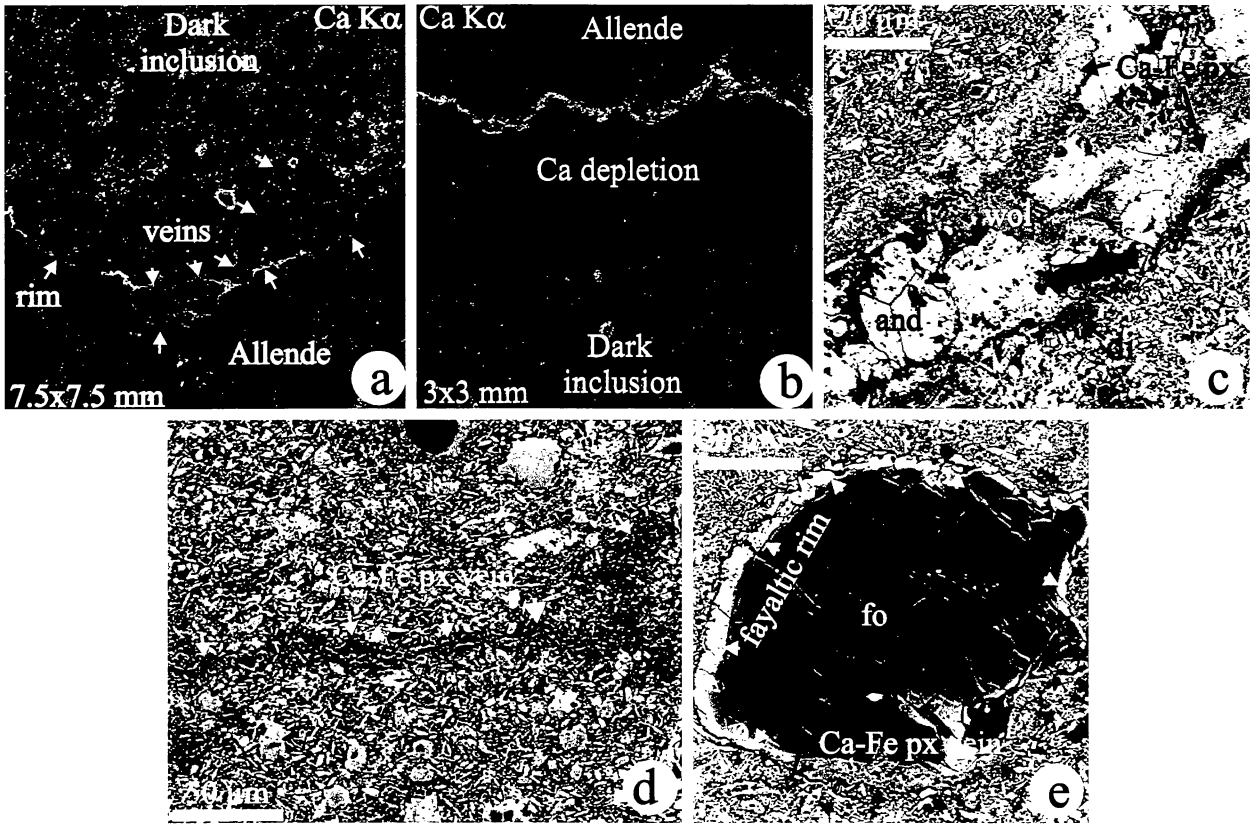

FIG. 11. X-ray elemental maps (a,b) and backscattered electron images (c–e) of the Allende dark inclusions. (a) Dark inclusion is surrounded by a Ca-rich rim and crosscut by Ca-rich veins. (b) A peripheral zone of the dark inclusion, surrounded by a Ca-rich rim, is depleted in Ca indicating mobilization of Ca to form the rim. (c) Ca-rich rim around Allende dark inclusion consists of Ca-Fe-rich pyroxenes (Ca-Fe px), diopside (di), andradite (and), and wollastonite (wol). The rim minerals show asymmetrical distribution. (d) Ca-Fe-rich pyroxene vein (marked by arrows) crosscutting the Allende-like matrix of the dark inclusion; the central part of the vein is empty. (e) An isolated forsterite (fo) grain is partly surrounded by a fayalitic olivine rim (marked by white arrows) and partly by a Ca-Fe-rich pyroxene vein (marked by black arrows). The absence of a continuous fayalitic olivine rim around forsterite may indicate that either the rim formation postdates formation of the vein or that the vein replaced the fayalitic olivine rim.

Allen *et al.*, 1978) in the pyroxene–andradite inclusions in matrices (Fig. 1) and in chondrules in the oxidized CV3 chondrites (Fig. 5a), which suggests similar conditions during their crystallization.

The crosscutting veins and the observed depletion in Ca of the exterior portions of the rimmed dark inclusions in Allende indicate that mobilization of Ca to form veins and rims took place after aggregation of the dark inclusions and after formation of the lath-shaped matrix olivines and fayalitic olivine rims around forsterite grains.

METAMORPHOSED CHONDRITIC CLASTS IN MOKOIA

In addition to the Kaba-like and Allende-like lithologies, the Mokoia breccia also contains relatively abundant (~5 vol%) chondritic clasts (<0.05–2 mm in size) consisting of Ca-rich fayalitic olivine ($Fa_{37\pm1}$, ~ 0.40 wt% CaO), Fe-rich Al-diopside ($Fs_{11}Wo_{49}$, ~4 wt% Al_2O_3), anorthitic plagioclase ($An_{46-81}Ab_{54-19}$), nepheline, Fe-rich Cr-spinel [$Fe_{tot}/(Fe_{tot} + Mg) = 0.68–0.77$, $Cr/(Cr + Al) = 0.26–0.41$, ~ 2.4 wt% TiO_2], Ni-poor pyrrhotite and pentlandite (22–28 wt% Ni), and rare grains of Ni-rich taenite (Cohen *et al.*, 1983; Krot and Hutcheon, 1997). Phyllosilicates are absent. The olivine and pyroxene grains, which are the major minerals in the clasts, typically form aggregates with 120° triple junctions indicating extensive recrystallization; chondrule textures (porphyritic and radial) can be distinguished in some cases. The apparent chondrule sizes, 1–2 mm, appear to be consistent with the CV3 range (Grossman *et al.*, 1988). Some of the granular materials around chondrules may represent metamorphosed matrix (Fig. 12b).

The textures and mineralogy of the clasts indicate that they were extensively metamorphosed above 750–800 °C (Krot and Hutcheon, 1997) prior to incorporation into the Mokoia breccia and after aqueous alteration of the host meteorite. The coexisting aluminum diopside, anorthitic plagioclase and chromium spinel and high CaO contents in olivine suggest that precursor material for the clasts was Ca- and Al-rich. The FeO-rich compositions of olivine and diopside, the absence of low-Ca pyroxenes and the mineralogy of the opaque assemblages suggest a high degree of oxidation. The mineralogy and mineral chemistry of the Mokoia clasts are unique among known metamorphosed ordinary and carbonaceous chondrites and achondrites (Krot and Hutcheon, 1997). They may be CV4/5 material that was excavated from the interior of the CV3 asteroid.

MOKOIA AND VIGARANO BRECCIAS: ARE ALL CV3 CHONDRITES FROM A SINGLE ASTEROID?

The oxidized CV3 chondrite breccia Mokoia and the reduced CV3 chondrite breccia Vigarano are known to contain solar-wind gases (Mazor *et al.*, 1970), suggesting that they are regolith breccias that can potentially provide information on the internal structure of the CV3 asteroidal body.

Although detailed textural observations of the Vigarano breccia are absent, there are several lines of evidence indicating that it

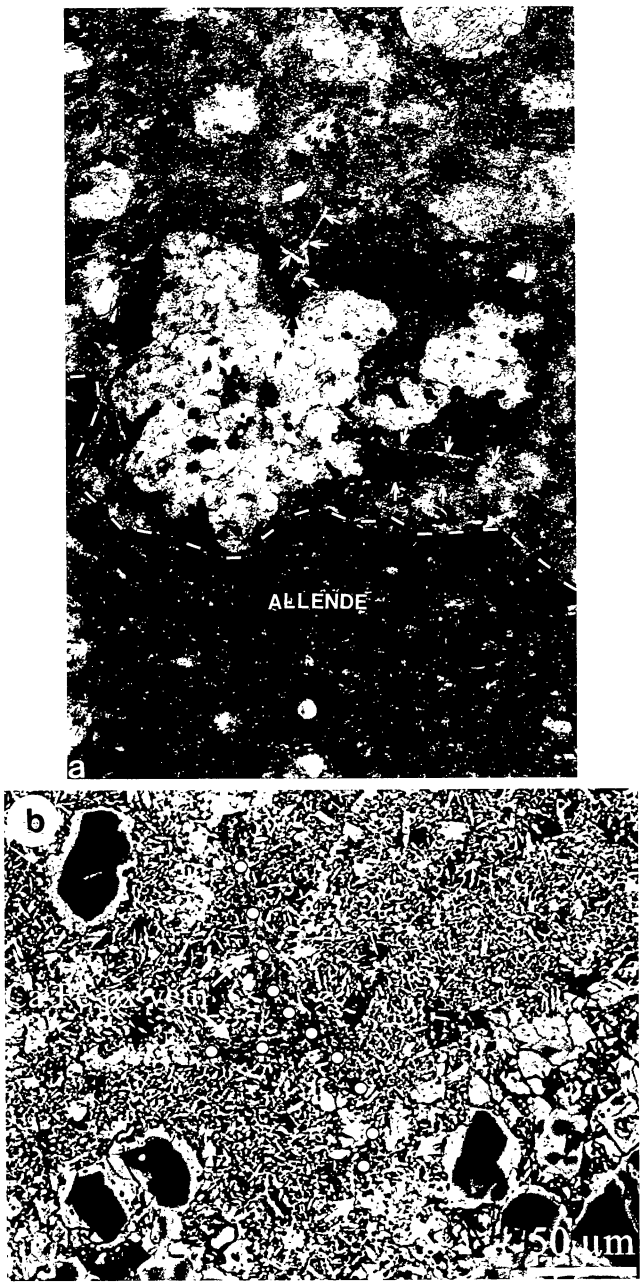

FIG. 12. Optical micrograph in transmitted light (a) and backscattered electron image (b) of a porhyritic olivine chondrule in the Allende dark inclusion. The boundary between Allende and the dark inclusion is indicated by a white dashed line. The chondrule is surrounded by a fine-grained rim consisting of lath-shaped fayalitic olivine and nepheline; it is crosscut by the Ca-Fe-rich pyroxene (indicated by arrows in top center in (a) and by dots in (b)) and fayalitic olivine veins (indicated by arrows in right center in (a)). The Ca-Fe-rich pyroxene vein starts at the opaque nodule in the chondrule (indicated by black arrow in (a) and by white arrows in (b)) that is replaced by Ca-Fe-rich pyroxenes and fayalitic olivine; sulfide grains (white in (b)) are relict.

contains both the reduced and oxidized components. McSween (1977) observed reduced and oxidized opaque assemblages. Some portions of the Vigarano matrix contain characteristic Allende-like features such as nepheline, sodalite, and magnetite (Peck, 1985; Graham and Lee, 1992), lath-shaped olivine morphology with relatively narrow compositional range (Fig. 10.2.6 in Scott *et al.*, 1988), and abundant Ca-Fe-rich pyroxene inclusions (Fig. 2).

Additional arguments come from chondrules and CAIs. Kimura and Ikeda (1996) found that many chondrules in Vigarano show alteration features similar to those in Allende: nepheline, sodalite, hedenbergite, fayalitic olivine rims around forsterite grains and fayalitic olivines replacing low-Ca pyroxene phenocrysts. Some CAIs in Vigarano experienced iron–alkali metasomatic alteration of melilite (Sylvester *et al.*, 1992, 1993; MacPherson and Davis, 1993). On the basis of these observations, we infer that Vigarano breccia contains the reduced and Allende-like lithologies.

The presence of the reduced and oxidized CV3 materials mixed in the Vigarano breccia and the presence of the Kaba-like and Allende-like lithologies in the Mokoia breccia suggest that all CV3 chondrites are from a single heterogeneously altered asteroidal body. The scale of mixing appears to be variable from centimeters to millimeters.

SUMMARY

The oxidized CV3 chondrites consist of two major subgroups or lithologies, Bali-like and Allende-like, which show characteristic alteration features in chondrules and matrices (Tables 1, 2 and 4). The $CV3_{oxB}$ lithology is present in Kaba, Bali, parts of the Mokoia breccia, and possibly, in Grosnaja and ALH 85006. It is characterized by the presence of phyllosilicates, magnetite, Ni-rich metal and sulfides, fayalite ($Fa_{>90}$), Ca-Fe-rich pyroxenes and andradite. The $CV3_{oxA}$ lithology observed in Allende, its dark inclusions, Axtell, ALHA81258, ALH 84028, LEW 86006, Mokoia and Vigarano breccias, contains abundant Ca-Fe-rich pyroxenes and andradite but virtually no fayalite or phyllosilicates. Instead, nepheline, sodalite and various textural types of fayalitic olivine (lath-shaped matrix olivine, fayalitic olivine rims around forsterite grains and fayalitic olivine replacing low-Ca pyroxenes) are common. Differences in the alteration features between Kaba-like and Allende-like lithologies reflect differences in the alteration conditions.

In the $CV3_{oxB}$ lithology, anorthitic mesostases and pyroxenes in chondrules and primary Ca-rich minerals in CAIs are replaced by low-Ca phyllosilicates (sodium phlogopite and saponite) suggesting mobilization of Ca during aqueous alteration. Magnetite nodules are replaced to various degrees by fayalite, Ca-Fe-rich pyroxenes and minor andradite. Some of the fayalite grains are corroded by Ca-Fe-rich pyroxenes. Fayalite associated with magnetite and sulfides forms veins, which crosscut chondrules and fine-grained rims and extend into the matrix. Oxygen isotopic compositions of the coexisting magnetite and fayalite in the Kaba-like chondrules in the Mokoia breccia plot close to the terrestrial fractionation line with large $\Delta^{18}O_{fayalite-magnetite}$ fractionation (~20‰). On the basis of the textural observations, O isotopic compositions of fayalite and magnetite, and thermodynamic analysis of the alteration reactions, we infer that phyllosilicates, magnetite, fayalite, Ca-Fe-rich pyroxenes and andradite formed at relatively low temperatures (<300 °C) by fluid–rock interaction in an asteroidal environment.

In the $CV3_{oxA}$ lithology, magnetite–sulfide nodules in chondrules and matrices are largely replaced by fayalitic olivine and Ca-Fe-rich pyroxenes; the latter are texturally and compositionally similar to those in the $CV3_{oxB}$ lithology suggesting a similar asteroidal origin. These Ca-Fe-rich pyroxenes predate the formation of lath-shaped matrix fayalitic olivines, fayalitic olivine rims around forsterites and fayalitic olivine replacing low-Ca pyroxenes in chondrules. Nepheline, sodalite and some Ca-rich phases (Ca-Fe-rich pyroxenes, wollastonite, andradite, and kirschsteinite) form veins in and rims

TABLE 4. Secondary mineralogy in chondrules in the reduced[1] and Bali-like[2] and Allende-like[3] subgroups of the CV3 chondrites and Allende dark inclusions.

	mgt	$FeNi_3$	pnt	$Fa_{>95}$	Ca-Fe pyx†	phyl‡	neph	sod	$Fa_{<50}$ halos	$Fa_{<50}$ others§	wo	andr	kir	gros
Reduced CV3s	–	–	–	–	–	–	–	–	–	–	–	–	–	–
Bali-like CV3s*	xx	xx	xx	xx	xx	xx	–	–	x	–	–	–	–	–
Allende-like CV3s	xx	xx	xx	–	xx	x/–	xx	xx	xx	xx	xx	xx	xx	xx
Allende dark incl.	x/–	x/–	xx	–	xx	–	x/–	xx	xx	xx	xx	xx	xx	xx

– = absent or rare, x = present, xx = common/abundant.
*Largely based on this study of chondrules in Kaba and Kaba-like portions of the Mokoia breccia.
†Ca–Fe pyroxenes replace magnetite nodules, contain minor andradite, vary in composition from $Fs_{10}Wo_{50}$ to $Fs_{50}Wo_{50}$.
‡Saponite and sodium phlogopite in the Bali-like subgroup; biopyriboles and talc in the Allende-like subgroup.
§Fayalitic olivine rims around forsterite grains and fayalitic olivine replacing low-Ca pyroxene grains.
Sources: 1 = Krot *et al.* (1995), Kimura and Ikeda (1996); 2 = Keller and Buseck (1990); this study; 3 = Ikeda and Kimura (1995, 1996, 1997), Kimura and Ikeda (1995, 1996, 1997), Brearley (1997a), Tomeoka and Buseck (1990); Cohen *et al.* (1983); Krot *et al.* (1995, 1997a); this study.
mgt = magnetite, pnt = pentlandite, pyx = pyroxene, phyl = phyllosilicates, neph = nepheline, sod = sodalite, wo = wollastonite, andr = andradite, kir = kirschsteinite, gros = grossular.

around CAIs and dark inclusions postdating formation of these textural types of fayalitic olivine.

Although the $CV3_{oxB}$ and $CV3_{oxA}$ lithologies have different major mineral carriers of Na (phyllosilicates and nepheline and sodalite, respectively), they have similar bulk Na contents. We infer that the $CV3_{oxA}$ lithology could have formed at higher temperatures, possibly from a $CV3_{oxB}$ lithology. The presence of nepheline-bearing veins crosscutting Allende dark inclusions (Tomeoka, 1997) and the observed depletion in bulk Na contents in most of the Allende dark inclusions (Bischoff *et al.*, 1988) supports mobilization of Na during fluid-assisted metamorphism. Because most of the Allende dark inclusions are depleted in Na, it seems plausible that Na lost from them was redistributed into the $CV3_{oxB}$ and $CV3_{oxA}$ lithologies of the oxidized CV3 chondrites.

We suggest that the secondary minerals in the oxidized CV3 chondrites resulted from fluid–rock interactions in the CV3 asteroid during progressive metamorphism of a heterogeneous mixture of ices and anhydrous materials mineralogically similar to the reduced CV3 chondrites. The presence of the $CV3_{oxA}$ lithology in the reduced breccia Vigarano and $CV3_{oxB}$ and $CV3_{oxA}$ lithologies in the Mokoia breccia suggest that all CV3 chondrites came from one heterogeneously altered asteroid. The metamorphosed clasts in Mokoia may be rare samples of the hotter interior of the CV asteroid.

Acknowledgments–We thank A. Brearley, X. Hua, M. Weisberg and J. T. Wasson for helpful discussions. We thank D. McGee for technical assistance with the scanning electron microscope and K. McKeegan for technical assistance with the ion probe. This work was supported in part by NASA grants NAG 5-4212 (K. Keil, P. I.), 152-11-40-23 (M. Zolensky, P. I.), NAGW 3451 (J. A. Wood, P. I.) and NSF grant EAR-9418520 (J. T. Wasson, P. I.). Access to the UCLA ion microprobe is supported through a grant from the NSF Instrumentation and Facilities program. This is HIGP publication number 1016 and SOEST publication number 4690.

Editorial handling: S. A. Sandford

REFERENCES

AKAI J. (1988) Incompletely transformed serpentine-type phyllosilicates in the matrix of Antarctic CM chondrites. *Geochim. Cosmochim. Acta* **52,** 1593–1599.

ALLEN J. M., GROSSMAN L., DAVIS A. M. AND HUTCHEON I. D. (1978) Mineralogy, textures and mode of formation of a hibonite-bearing Allende inclusion. *Proc. Lunar Planet. Sci. Conf.* **9th,** 1209–1233.

BISCHOFF A., PALME H., SPETTEL B., CLAYTON R. N. AND MAYEDA T. K. (1988) The chemical composition of dark inclusions from the Allende meteorite (abstract). *Lunar Planet. Sci.* **19,** 88–89.

BLUM J. D., WASSERBURG G. J., HUTCHEON I. D., BECKETT J. R. AND STOLPER E. M. (1989) Origin of opaque assemblages in CV3 meteorites: Implications for nebular and planetary processes. *Geochim. Cosmochim. Acta* **53,** 543–556.

BREARLEY A. J. (1996) A comparison of FeO-rich olivines in chondrules, matrix, and dark inclusions in Allende, and the discovery of phyllosilicate veins in chondrule enstatite (abstract). *Meteorit. Planet. Sci* **31 (Suppl.),** A21–A22.

BREARLEY A. J. (1997a) Disordered biopyriboles and talc in chondrules in the Allende meteorite: Possible origins and formation conditions (abstract). *Lunar Planet. Sci.* **28,** 153–154.

BREARLEY A. J. (1997b) Contrasting microstructures of fayalitic olivine in matrix and chondrules in the Allende CV3 chondrite (abstract). *Lunar Planet. Sci.* **28,** 151–152.

BREARLEY A. J. AND PRINZ M. (1996) Dark inclusions in the Allende meteorite: New insights from transmission electron microscopy (abstract). *Lunar Planet. Sci.* **27,** 161–162.

CHOI B-G., MCKEEGAN K. D., LESHIN L. A. AND WASSON J. T. (1997) Origin of magnetite in oxidized CV chondrites: *In situ* measurement of oxygen isotope compositions of Allende magnetite and olivine. *Earth Planet. Sci. Lett.* **146,** 337–349.

CLAYTON R. N. (1993) Oxygen isotopes in meteorites. *Ann. Rev. Earth Planet. Sci.* **21,** 115–149.

CLAYTON R. N. (1997) Use of oxygen isotopes to constrain the nebular and asteroidal modification of chondritic materials (abstract). In *Workshop on Parent-Body and Nebular Modification of Chondritic Materials* (eds. M. E. Zolensky, A. N. Krot and E. R. D. Scott), pp. 10–11. LPI Tech. Rep. No. **97-02,** Part 1, Lunar and Planetary Institute, Houston, Texas, USA.

CLAYTON R. N. AND MAYEDA T. K. (1984) The oxygen isotope record in Murchison and other carbonaceous chondrites. *Earth Planet. Sci. Lett.* **67,** 151–161.

CLAYTON R. N. AND MAYEDA T. K. (1996) Oxygen isotope relations among CO, CK, and CM chondrites and carbonaceous chondrite dark inclusions (abstract). *Meteorit. Planet. Sci* **31 (Suppl.),** A30.

CLAYTON R. N., MAYEDA T. K., PALME H. AND LAUGHLIN J. (1986) Oxygen, silicon, and magnesium isotopes in Leoville refractory inclusions (abstract). *Lunar Planet. Sci.* **17,** 139–140.

CLAYTON R. N., MAYEDA T. K., MACPHERSON G. J. AND GROSSMAN L. (1987) Oxygen and silicon isotopes in inclusions and chondrules from Vigarano (abstract). *Lunar Planet. Sci.* **18,** 185–186.

CLAYTON R. N., MAYEDA T. K., KOJIMA H., WEISBERG M. K. AND PRINZ M. (1997) Hydration and dehydration in carbonaceous chondrites (abstract). *Lunar Planet. Sci.* **28,** 239–240.

COHEN R. E., KORNACKI A. S. AND WOOD J. A. (1983) Mineralogy and petrology of chondrules and inclusions in the Mokoia CV3 chondrite. *Geochim. Cosmochim. Acta* **47,** 1739–1757.

DOHMEN R., CHAKRABORTY S., PALME H. AND RAMMENSEE W. (1997) High-temperature formation of iron-oxide-rich olivine in the early solar system: Experimental simulation with thermodynamic and kinetic analysis of a solid-solid reaction mediated by a gas phase (abstract). *Meteorit. Planet. Sci* **32 (Suppl.),** A35–A36.

FEGLEY B. (1997) Theoretical models and experimental studies of gas-grain chemistry in the solar nebula (abstract). In *Workshop on Parent-Body and Nebular Modification of Chondritic Materials* (eds. M. E. Zolensky, A. N. Krot and E. R. D. Scott), pp. 14–15. LPI Tech. Rep. No. **97-02,** Part 1, Lunar and Planetary Institute, Houston, Texas, USA.

GRAHAM A. L. AND LEE M. (1992) The matrix mineralogy of the Vigarano (CV3) chondrite (abstract). *Lunar Planet. Sci.* **23,** 435–436.

GRESHAKE A. (1997) Primitive matrix components of the unique carbonaceous chondrite Acfer 094: Clues to their origin. In *Workshop on Parent-Body and Nebular Modification of Chondritic Materials* (eds. M. E. Zolensky, A. N. Krot and E. R. D. Scott), pp. 18–19. LPI Tech. Rep. No. **97-02,** Part 1, Lunar and Planetary Institute, Houston, Texas, USA.

GRIMM R. E. AND MCSWEEN H. Y. (1989) Water and the thermal evolution of carbonaceous chondrite parent bodies. *Icarus* **82,** 244–280.

GROSSMAN J. N, RUBIN A. E., NAGAHARA H. AND KING E. A. (1988) Properties of chondrules. In *Meteorites and the Early Solar System.* (eds. J. F. Kerridge and M. S. Matthews), pp. 619–659. Univ. Arizona Press, Tucson, Arizona, USA.

HAGGERTY S. E. AND MCMAHON B. M. (1979) Magnetite-sulfide-metal complexes in the Allende meteorite. *Proc. Lunar Planet. Sci. Conf.* **10th,** 851–870.

HASHIMOTO A. AND GROSSMAN L. (1987) Alteration of Al-rich inclusions inside amoeboid olivine aggregates in the Allende meteorite. *Geochim. Cosmochim. Acta* **51,** 1685–1704.

HAYATSU R., WINANS R. E., SCOTT R. G., MCBETH R. L., MOORE L. P. AND STUDIER M. H. (1980) Phenolic ethers in the organic polymer of the Murchison meteorite. *Science* **207,** 1202–1204.

HOUSLEY R. M. AND CIRLIN E. H. (1983) On the alteration of Allende chondrules and the formation of matrix. In *Chondrules and Their Origins* (ed. E. D. King), pp. 145–161. Lunar and Planetary Institute, Houston, Texas, USA.

HUA X. AND BUSECK P. R. (1995) Fayalite in the Kaba and Mokoia carbonaceous chondrites. *Geochim. Cosmochim. Acta* **59,** 563–579.

HUA X. AND BUSECK P. R. (1997) Fayalitic halos within forsterites from carbonaceous chondrites (abstract). In *Workshop on Parent-Body and Nebular Modification of Chondritic Materials* (eds. M. E. Zolensky, A. N. Krot and E. R. D. Scott), pp. 26–27. LPI Tech. Rep. No. **97-02,** Part 1, Lunar and Planetary Institute, Houston, Texas, USA.

HUA X., ADAM J., PALME H. AND EL GORESY A. (1988) Fayalite-rich rims, veins, and halos around and in forsteritic olivines in CAIs and chondrules in carbonaceous chondrites: Types, compositional profiles and constraints of their formation. *Geochim. Cosmochim. Acta* **52,** 1389–1408.

IKEDA Y. AND KIMURA M. (1995) Anhydrous alteration of Allende chondrules in the solar nebula I: Description and alteration of chondrules with known oxygen-isotopic compositions. *Proc. NIPR Symp. Antarct. Meteorites* **8,** 97–122.

IKEDA Y. AND KIMURA M. (1996) Anhydrous alteration of Allende chondrules in the solar nebula III: Alkali-zoned chondrules and heating experiments for anhydrous alteration. *Proc. NIPR Symp. Antarct. Meteorites* **9,** 51–68.

IKEDA Y. AND KIMURA M. (1997) Anhydrous alteration of Allende chondrules in the solar nebula (abstract). In *Workshop on Parent-Body and Nebular Modification of Chondritic Materials* (eds. M. E. Zolensky, A. N. Krot and E. R. D. Scott), pp. 29–30. LPI Tech. Rep. No. **97-02,** Part 1, Lunar and Planetary Institute, Houston, Texas, USA.

JOHNSON C. A., PRINZ M., WEISBERG M. K., CLAYTON R. N. AND MAYEDA T. K. (1990) Dark inclusions in Allende, Leoville, and Vigarano: Evidence for nebular oxidation of CV3 constituents. *Geochim. Cosmochim. Acta* **54,** 819–831.

KELLER L. P. (1997) A transmission electron microscope study of the matrix mineralogy of the Leoville CV3 (reduced-group) carbonaceous chondrite: Nebular and parent-body features (abstract). In *Workshop on Parent-Body and Nebular Modification of Chondritic Materials* (eds. M. E. Zolensky, A. N. Krot and E. R. D. Scott), pp. 31–33. LPI Tech. Rep. No. **97-02,** Part 1, Lunar and Planetary Institute, Houston, Texas, USA.

KELLER L. P. AND BUSECK P. R. (1989) Alteration of Ca- and Al-rich inclusions in Allende: A transmission electron microscope study (abstract). *Lunar Planet. Sci.* **20,** 512–513.

KELLER L. P. AND BUSECK P. R. (1990) Aqueous alteration in the Kaba CV3 carbonaceous chondrite. *Geochim. Cosmochim. Acta* **54,** 2113–2120.

KELLER L. P. AND MCKAY D. S. (1993) Aqueous alteration of the Grosnaja CV3 carbonaceous chondrite (abstract). *Meteoritics* **28,** 378.

KELLER L. P., THOMAS K. L., CLAYTON R. N., MAYEDA T. K., DEHART J. M. AND MCKAY D. S. (1994) Aqueous alteration of the Bali CV3 chondrite: Evidence from mineralogy, mineral chemistry, and oxygen isotopic compositions. *Geochim. Cosmochim. Acta* **58,** 5589–5598.

KIMURA M. AND IKEDA Y. (1995) Anhydrous alteration of Allende chondrules in the solar nebula II: Alkali-Ca exchange reactions and formation of nepheline, sodalite and Ca-rich phases in chondrules. *Proc. NIPR Symp. Antarct. Meteorites* **8,** 123–138.

KIMURA M. AND IKEDA Y. (1996) Comparative study on alteration processes of chondrules in oxidized and reduced CV3 chondrites (abstract). *Meteorit. Planet. Sci.* **31 (Suppl.),** A70–A71

KIMURA M. AND IKEDA Y. (1997) Relationship between anhydrous and aqueous alterations in CV3 chondrites (abstract). In *Workshop on Parent-Body and Nebular Modification of Chondritic Materials* (eds. M. E. Zolensky, A. N. Krot and E. R. D. Scott), pp. 33–34. LPI Tech. Rep. No. **97-02,** Part 1, Lunar and Planetary Institute, Houston, Texas, USA.

KOJIMA T. AND TOMEOKA K. (1994) Evidence for aqueous alteration and thermal metamorphism in a dark clast found in Allende (abstract). *Meteoritics* **29**, 484.

KOJIMA T. AND TOMEOKA K. (1996) Indicators of aqueous alteration and thermal metamorphism on the CV3 parent body: Microtextures of a dark inclusion from Allende. *Geochim. Cosmochim. Acta* **60,** 2651–2666.

KOJIMA T., TOMEOKA K. AND TAKEDA H. (1993) Unusual dark clasts in the Vigarano CV3 carbonaceous chondrite: Record of parent body process. *Meteoritics* **28,** 649–658.

KRACHER A., KEIL K., KALLEMEYN G. W., WASSON J. T. AND CLAYTON R. N. (1985) The Leoville (CV3) accretionary breccia. *Proc. Lunar Planet. Sci. Conf.* **16th,** D123–D135.

KROT A. N. AND HUTCHEON I. D. (1997) Highly-oxidized and metamorphosed chondritic or igneous (?) clasts in the CV3 carbonaceous chondrite Mokoia: Excavated material from the interior of the CV3 asteroid or previously unsampled asteroid (abstract). *Lunar Planet. Sci.* **28**, 767–768.

KROT A. N., SCOTT E. R. D. AND ZOLENSKY M. E. (1995) Mineralogical and chemical modification of components in CV3 chondrites: Nebular or asteroidal processing? *Meteoritics* **30,** 748–776.

KROT A. N., ZOLENSKY M. E., SCOTT E. R. D. AND KEIL K. (1996) Asteroidal formation of Ca-Fe-Mg silicates in Allende dark inclusions, Allende host and other oxidized CV3 chondrites (abstract). *Meteorit. Planet. Sci.* **31 (Suppl.),** A74–A75.

KROT A. N., SCOTT E. R. D. AND ZOLENSKY M. E. (1997a) Origin of fayalitic olivine rims and lath-shaped matrix olivine in the CV3 chondrite Allende and its dark inclusions. *Meteorit. Planet. Sci* **32,** 31–49.

KROT A. N., ZOLENSKY M. E., CHOI B-G., PETAEV M. I., KEIL K., SCOTT E. R. D. AND WASSON J. T. (1997b) Metasomatism and metamorphism in the CV3 asteroid: Formation of pure fayalite, diopside-hedenbergite pyroxenes, andradite, and magnetite in Kaba and Mokoia (abstract). *Meteorit. Planet. Sci* **32 (Suppl.),** A74–A75.

KROT A. N., BREARLEY A. J., BIRYUKOV V. V., ULYANOV A. A., KEIL K., SWINDLE T. D. AND MITTLEFEHLDT D. W. (1997c) Dark inclusions in the reduced CV3 chondrite Efremovka: Evidence for various degrees of aqueous alteration and thermal metamorphism (abstract). *Lunar Planet. Sci.* **28,** 769–770.

KROT A. N., SCOTT E. R. D. AND ZOLENSKY M. E. (1997d) Mineralogical and chemical modification of CV3 chondrites during fluid-assisted metamorphism in the CV3 asteroid (abstract). In *Workshop on Parent-Body and Nebular Modification of Chondritic Materials* (eds. M. E. Zolensky, A. N. Krot and E. R. D. Scott), pp. 34–36. LPI Tech. Rep. No. **97-02,** Part 1, Lunar and Planetary Institute, Houston, Texas, USA.

KROT A. N., PETAEV M. I., ZOLENSKY M. E., KEIL K., SCOTT E. R. D. AND NAKAMURA K. (1998a) Secondary calcium-iron-rich minerals in the Bali-like and Allende-like oxidized CV3 chondrites and Allende dark inclusions. *Meteorit. Planet. Sci.* **33,** 623–645.

KROT A. N., BREARLEY A. J., ULYANOV A. A., BIRYUKOV V. V., SWINDLE T. D., KEIL K., MITTLEFEHLDT D. W., CLAYTON R. N. AND MAYEDA T. K. (1998b) Mineralogy, petrography, bulk chemical, I-Xe and oxygen isotope compositions of the dark inclusions in the reduced CV3 chondrite Efremovka: Evidence for various degrees of aqueous alteration and thermal metamorphism. *Meteorit. Planet. Sci.* **33,** in press.

KURAT G., PALME H., BRANDSTÄTTER F. AND HUTH J. (1989) Allende xenolith AF: Undistirbed record of condensation and aggregation of matter in the solar nebula. *Z. Naturforsch.* **44a**, 988–1004.

LAURETTA D. S., LODDERS K. AND FEGLEY B., JR. (1997) Experimental simulations of sulfide formation in the solar nebula. *Science* **277,** 358–360.

MACPHERSON G. J. AND DAVIS A. M. (1993) A petrologic and ion microprobe study of a Vigarano Type B refractory inclusion: Evolution by multiple stages of alteration and melting. *Geochim. Cosmochim. Acta* **57,** 231–243.

MACPHERSON G. J. AND DAVIS A. M. (1997) Parent-body metamorphism of CV3 chondrites: Counterarguments based on accretionary rims and calcium-aluminum-rich inclusions (abstract). In *Workshop on Parent-Body and Nebular Modification of Chondritic Materials* (eds. M. E. Zolensky, A. N. Krot and E. R. D. Scott), pp. 42–43. LPI Tech. Rep. No. **97-02,** Part 1, Lunar and Planetary Institute, Houston, Texas, USA.

MACPHERSON G. J., GROSSMAN L., ALLEN J. M. AND BECKETT J. R. (1981) Origin of rims on coarse-grained inclusions in the Allende meteorite. *Proc. Lunar Planet. Sci. Conf.* **12B,** 1079–1091.

MacPherson G. J., Hashimoto A. and Grossman L. (1985) Accretionary rims on inclusions in the Allende meteorite. *Geochim. Cosmochim. Acta* **49,** 2267–2279.

MacPherson G. J., Wark D. A. and Armstrong J. T. (1988) Primitive material surviving in chondrites: Refractory inclusions. In *Meteorites and the Early Solar System* (eds. J. F. Kerridge and M. S. Matthews), pp. 746–807. Univ. Arizona Press, Tucson, Arizona, USA.

Mazor E., Heymann D. and Anders E. (1970) Noble gases in carbonaceous chondrites. *Geochim. Cosmochim. Acta* **34,** 781–824.

McGuire A. V. and Hashimoto A. (1989) Origin of zoned fine-grained inclusions in the Allende meteorite. *Geochim. Cosmochim. Acta* **1989,** 1123–1133.

McMahon B. M. and Haggerty S. E. (1980) Experimental studies bearing on the magnetite-alloy-sulfide association in the Allende meteorite: Constraints on the conditions of chondrule formation. *Proc. Lunar Planet. Sci. Conf.* **11th,** 1003–1025.

McSween H. Y. (1977) Petrographic variations among carbonaceous chondrites of the Vigarano type. *Geochim. Cosmochim. Acta* **41,** 1777–1790.

Nakamura T., Tomeoka K. and Takeda H. (1992) Shock effects of the Leoville CV carbonaceous chondrite: A transmission electron microscope study. *Earth Planet. Sci. Lett.* **114,** 159–170.

Naumov G. B., Ryzhenko B. N. and Khodakovski Y. L. (1971) *Handbook of Thermodynamic Quantities for Geology* (in Russian). Atomic Press, Moscow, Russia. 240 pp.

Palme H. (1997) Oxygen-fugacity indicators in carbonaceous chondrites: Parent-body alteration or high-temperature nebular oxidation (abstract). In *Workshop on Parent-Body and Nebular Modification of Chondritic Materials* (eds. M. E. Zolensky, A. N. Krot and E. R. D. Scott), pp. 48–49. LPI Tech. Rep. No. **97-02,** Part 1, Lunar and Planetary Institute, Houston, Texas, USA.

Palme H. and Fegley B. (1990) High-temperature condensation of iron-rich olivine in the solar nebula. *Earth Planet. Sci. Lett.* **101,** 180–195.

Palme H. and Wark D. A. (1988) CV-chondrites: High-temperature gas-solid equilibrium *vs.* parent body metamorphism (abstract). *Lunar Planet. Sci.* **19,** 897–898.

Palme H., Larimer J. W. and Lipschutz M. E. (1988) Moderately volatile elements. In *Meteorites and The Early Solar System* (eds. J. F. Kerridge and M. S. Matthews), pp. 436–462. Univ. Arizona Press, Tucson, Arizona, USA.

Palme H., Kurat G., Spettel B. and Burghele A. (1989) Chemical composition of an unusual xenolith of the Allende meteorite. *Z. Naturforsch.* **44a,** 1005–1014.

Peck J. A. (1985) Mineralogy and chemistry of CV3 chondrite matrix: Clues to processes in the early solar nebula. Bachelor dissertation, Harvard University. 123 pp.

Peck J. A. and Wood J. A. (1987) The origin of ferrous zoning in Allende chondrule olivine. *Geochim. Cosmochim. Acta* **51,** 1503–1510.

Petaev M. I. and Mironenko M. V. (1997) Thermodynamic modeling of aqueous alteration in CV chondrites (abstract). In *Workshop on Parent-Body and Nebular Modification of Chondritic Materials* (eds. M. E. Zolensky, A. N. Krot and E. R. D. Scott), pp. 49–50. LPI Tech. Rep. No. **97-02,** Part 1, Lunar and Planetary Institute, Houston, Texas, USA.

Rubin A. E. (1991) Euhedral awaruite in the Allende meteorite: Implications for the origin of awaruite- and magnetite-bearing nodules in CV3 chondrites. *Am. Mineral.* **76,** 1356–1362.

Rubin A. E., Fegley B. and Brett R. (1988) Oxidation state in chondrites. In *Meteorites and the Early Solar System* (eds. J. F. Kerridge and M. S. Matthews), pp. 488–511. Univ. Arizona Press, Tucson, Arizona, USA.

Scott E. R. D., Barber D. J., Alexander C. M. O., Hutchison R. and Peck J. A. (1988) Primitive material surviving in chondrites; Matrix. In *Meteorites and the Early Solar System* (eds. J. F. Kerridge and M. S. Matthews), pp. 718–745. Univ. Arizona Press, Tucson, Arizona, USA.

Scott E. R. D., Keil K. and Stöffler D. (1992) Shock metamorphism of carbonaceous chondrites. *Geochim. Cosmochim. Acta* **56,** 4281–4293.

Simon S. B., Grossman L., Casanova I., Symes S., Benoit P., Sears D. W. G. and Wacker J. F. (1994) Axtell, a new CV3 chondrite find from Texas. Meteoritics **30,** 42–46.

Sylvester P. J., Grossman L. and MacPherson G. J. (1992) Refractory inclusions with unusual chemical compositions from the Vigarano carbonaceous chondrite. *Geochim. Cosmochim. Acta* **56,** 1343–1363.

Sylvester P. J., Simon S. B. and Grossman L. (1993) Refractory inclusions from the Leoville, Efremovka, and Vigarano C3V chondrites: Major element differences between Type A and B, and extraordinary refractory siderophile element compositions. *Geochim. Cosmochim. Acta* **57,** 3763–3784.

Tomeoka K. (1997) Aqueous alteration and dehydration processes in the carbonaceous chondrites (abstract). In *Workshop on Parent-Body and Nebular Modification of Chondritic Materials* (eds. M. E. Zolensky, A. N. Krot and E. R. D. Scott), pp. 61–62. LPI Tech. Rep. No. **97-02,** Part 1, Lunar and Planetary Institute, Houston, Texas, USA.

Tomeoka K. and Buseck P. R. (1982a) Intergrown mica and montmorillonite in the Allende carbonaceous chondrite. *Nature* **299,** 326–327.

Tomeoka K. and Buseck P. R. (1982b) An unusual layered mineral in chondrules and aggregates of the Allende carbonaceous chondrite. *Nature* **299,** 327–329.

Tomeoka K. and Buseck P. R. (1990) Phyllosilicates in the Mokoia CV carbonaceous chondrite: Evidence for aqueous alteration in an oxidizing condition. *Geochim. Cosmochim. Acta* **54,** 1745–1754.

Weinbruch S., Palme H., Müller W. F. and El Goresy A. (1990) FeO-rich rims and veins in Allende forsterite: Evidence for high temperature condensation at oxidizing conditions. *Meteoritics* **25,** 115–125.

Weinbruch S., Zinner E. K., El Goresy A., Steele A. and Palme H. (1993) Oxygen isotopic composition of individual olivine grains from the Allende meteorite. *Geochim. Cosmochim. Acta* **57,** 2649–2661.

Weisberg M. K. and Prinz M. (1997) Fayalitic olivine in CV3 chondrite matrix and dark inclusions: A nebular origin (abstract). In *Workshop on Parent-Body and Nebular Modification of Chondritic Materials* (eds. M. E. Zolensky, A. N. Krot and E. R. D. Scott), pp. 66–67. LPI Tech. Rep. No. **97-02,** Part 1, Lunar and Planetary Institute, Houston, Texas, USA.

Weisberg M. K., Prinz M. E., Boesenberg S., Kozhushko G., Clayton R. N., Mayeda T. K. and Ebihara M. E. (1996) A petrologic and oxygen isotopic study of six Allende dark inclusions: Evaluation of nebular *vs.* Asteroidal models for their origin (abstract). *Lunar Planet. Sci.* **27,** 1407–1408.

Weisberg M. K., Prinz M., Clayton R. N. and Mayeda T. K. (1997) CV3 chondrites: Three subgroups, not two (abstract). *Meteorit. Planet. Sci.* **32 (Suppl.),** A138–A139.

Wood J. A. and Hashimoto A. (1993) Mineral equilibrium in fractionated nebular systems. *Geochim. Cosmochim. Acta* **57,** 2377–2388.

Zolensky M. E. and Krot A. N. (1996) Mineralogical and compositional study of an Allende dark inclusions (abstract). *Lunar Planet. Sci.* **27,** 1503–1504.

APPENDIX

ARGUMENTS AGAINST AN ASTEROIDAL ALTERATION MODEL

In this section, we discuss some arguments presented at the Workshop on Parent-Body and Nebular Modification of Chondritic Materials against the asteroidal model of alteration of CV3 chondrites. Some criticism was directed against the idea that the Allende matrix was completely hydrated and subsequently dehydrated to form fayalitic olivine (*e.g.*, Clayton, 1997; Weisberg *et al.*, 1997; Palme, 1997). Because the asteroidal model described above only requires partial alteration in the presence of an aqueous solution, we will focus our discussion on the other counterarguments. We also discuss some limitations of bulk O isotopic compositions of CV3 chondrites for understanding their alteration history.

Multilayered "Accretionary" Rims around Allende Calcium-Aluminum-rich Inclusions

Calcium-aluminum-rich inclusions in Allende and Vigarano are commonly surrounded by multilayered porous rims, with layers differing in mineral proportions, grain size and mineral chemistry (MacPherson *et al.*, 1985; MacPherson and Davis, 1997). The rims consist of fayalitic olivines (most of them lath shaped), andradite, nepheline, sodalite, and Ca-Fe-rich pyroxenes, which vary in composition from diopside to hedenbergite. MacPherson and co-workers note that minerals, such as nepheline and sodalite, are confined to specific rims' layers and conclude that these rims formed by sequential accretion of mineral grains that condensed from the solar nebula gas. We agree that these minerals do not replace specific minerals *in situ*. However, we note that there is much evidence that Ca-Fe-rich pyroxenes, andradite and wollastonite in the outermost rims around CAIs in Allende formed by metasomatic alteration of the CAIs (MacPherson *et al.*, 1981; McGuire and Hashimoto, 1989).

We infer that lath-shaped fayalitic olivines, andradite, nepheline, sodalite, and Ca-Fe-rich pyroxenes in these rims are secondary minerals formed by metasomatic alteration of CAIs that were surrounded by fine-grained accretionary rims of matrix material. The matrix material may have originally resembled the matrix in the reduced CV chondrites, or possibly that in Acfer-094 (Table 2). The Ca-Fe-rich silicates, nepheline and sodalite

formed specific layers in the rimmed CAIs because of chemical gradients established between the major decomposing minerals in the CAIs such as melilite and the aqueous solution that percolated through the surrounding porous matrix. Based on our study of the Ca-rich veins in and rims around the Allende dark inclusions consisting of the Ca-Fe-rich pyroxenes, wollastonite, and andradite (Krot *et al.*, 1996), we infer that the metasomatic alteration of the Allende CAIs took place in an asteroidal environment. Because similar secondary minerals are present in altered chondrules in the Allende-like meteorites (*e.g.*, Ikeda and Kimura, 1997), we expect to find analogous layered rims on some altered chondrules.

MacPherson and Davis (1997) inferred that "whiskers of wollastonite found within cavities in CAIs formed at low degrees of supersaturation from a vapor which is difficult to reconcile with parent-body metamorphism." However, we conclude that the presence of wollastonite needles in porous Ca-rich rims around dark inclusions in Allende suggests that these whiskers can form during parent body metamorphism (Krot *et al.*, 1996, 1998a).

MacPherson and Davis (1997) also argue that the disequilibrium mineral assemblages and fine-scale zoning of minerals "could not have survived extensive high-temperature parent-body metamorphism of the type proposed by Krot *et al.* (1995)." We agree that peak metamorphic temperatures in Allende (<400–500 °C) were not high enough to allow diffusion over distances more than a few microns in olivine and less than a micron in pyroxene. The presence of strongly zoned olivines 10–20 μm in size and the apparent direct contact of diopside and hedenbergite are not incompatible with our proposed metamorphic history.

Brecciation and Alteration

One of the commonly used arguments against the asteroidal model of alteration of CV3 chondrites is the presence of unaltered materials in direct contact with the secondary minerals (*e.g.*, Hua *et al.*, 1988; Weinbruch *et al.*, 1990; Weisberg *et al.*, 1997; Ikeda and Kimura, 1997). We infer that typically the alteration did not occur *in situ* but predated brecciation. The observed replacement of nepheline by phyllosilicates in the Mokoia breccia may indicate that the aqueous alteration continued during brecciation or that it was episodic.

Oxygen Isotopic Compositions

Oxygen isotopes provide a powerful tool for study of hydration and dehydration reactions and were successfully used for modeling of the relatively low-temperature (0–25 °C) aqueous alteration of CM chondrites (Clayton and Mayeda, 1984; Clayton, 1997; Clayton *et al.*, 1997). Recently, Clayton and Mayeda (1996) showed that CK, CO and CM chondrites fall along a slope of ~0.7 on a three-O isotope plot that appears to be a mixing line between an ^{16}O-rich component (anhydrous high-temperature silicates) and ^{16}O-poor component (low-temperature phyllosilicates or their dehydration products). In contrast, bulk O isotopic compositions of Allende dark inclusions and CV chondrites, including aqueously altered Kaba, Bali, and Mokoia, plot close to the Allende CAI line with a slope of ~0.95 (Fig. 14), which is generally attributed to high-temperature isotopic exchange reactions between ^{16}O-rich solids and ^{16}O-poor solar nebula gas (*e.g.*, Clayton and Mayeda, 1984; Clayton, 1993).

Bulk O isotopic compositions of the separated matrix samples in the aqueously altered Kaba and Mokoia and anhydrous Allende are similarly depleted in ^{16}O with respect to the bulk compositions of their hosts and plot along the 0.95 slope line (Weisberg *et al.*, 1997). The unaltered and heavily aqueously altered portions of Bali show a similar but more pronounced effect (Keller *et al.*, 1994), and the same trend is shown by Allende dark inclusions that have been altered to various degrees (Krot *et al.*, 1995). However, there is no simple relationship between δ^{17}O and the extent of alteration (Palme, 1997). Some of the observed bulk O isotopic compositional variations within the CV3 group are probably due to sample heterogeneity resulting from large sizes of chondrules and CAIs with significantly different O isotopic compositions. As a result, even relatively unaltered CV3 chondrites of the reduced subgroup (Leoville and Efremovka) show variations in bulk O isotopic compositions that are comparable to those between heavily altered and slightly altered portions of Bali (Fig. 13). We conclude that the degree of hydration of CV3 chondrites can not be estimated from bulk O isotopic data.

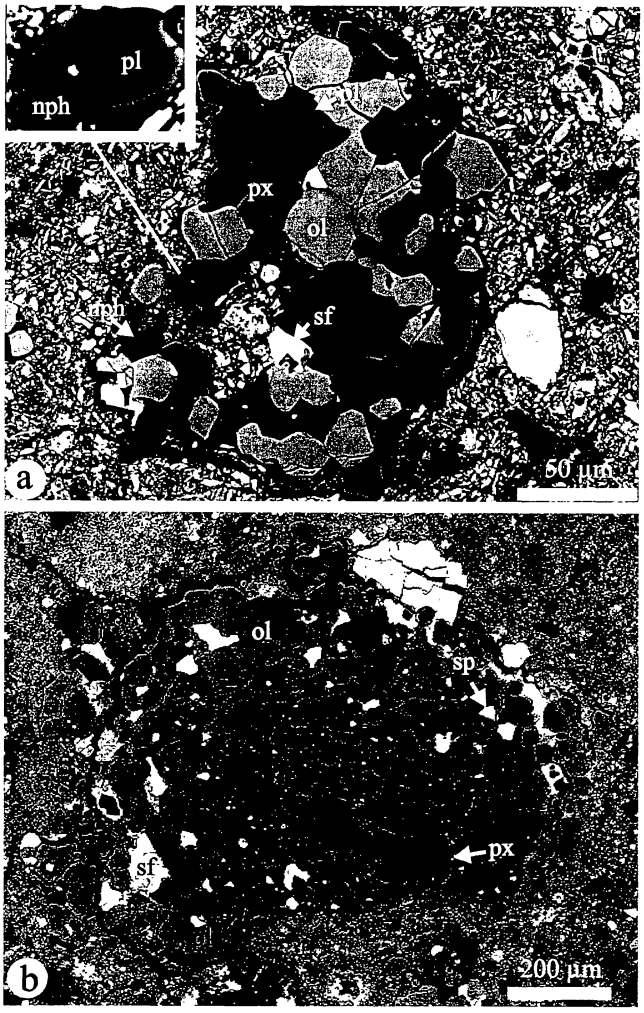

FIG. 13. (a,b) Backscattered electron images of heavily metamorphosed chondritic clasts in the Mokoia breccia. The clasts have granular (a) and radial (b) textures and consist of fayalitic olivine (ol), Fe-rich diopside (px), anorthitic plagioclase (pl), nepheline (nph), Cr-spinel (sp), pyrrhotite, pentlandite (sf) and Ni-rich metal. Olivine, pyroxene and plagioclase grains form aggregates with 120° triple junctions. The granular material around the chondrule in (b) and in the clast in (a) may be metamorphosed matrix material.

From these observations, we infer that aqueous alteration of CV chondrites resulted in their enrichment in ^{17}O and ^{18}O but did not shift significantly their bulk O isotopic compositions off the Allende CAI line. The observed differences between CK-, CO-, CM and CV-Allende dark inclusions' bulk O isotopic composition trends may indicate different conditions of aqueous alteration (*e.g.*, lower water to rock ratio in the CV3 asteroid, Clayton and Mayeda, 1996; Krot *et al.*, 1997a; higher temperature of alteration of CV3 chondrites, R. N. Clayton, pers. comm.; Krot *et al.*, 1997a; or different O isotopic composition of water that accreted into the CV3 asteroid, Krot *et al.*, 1997a).

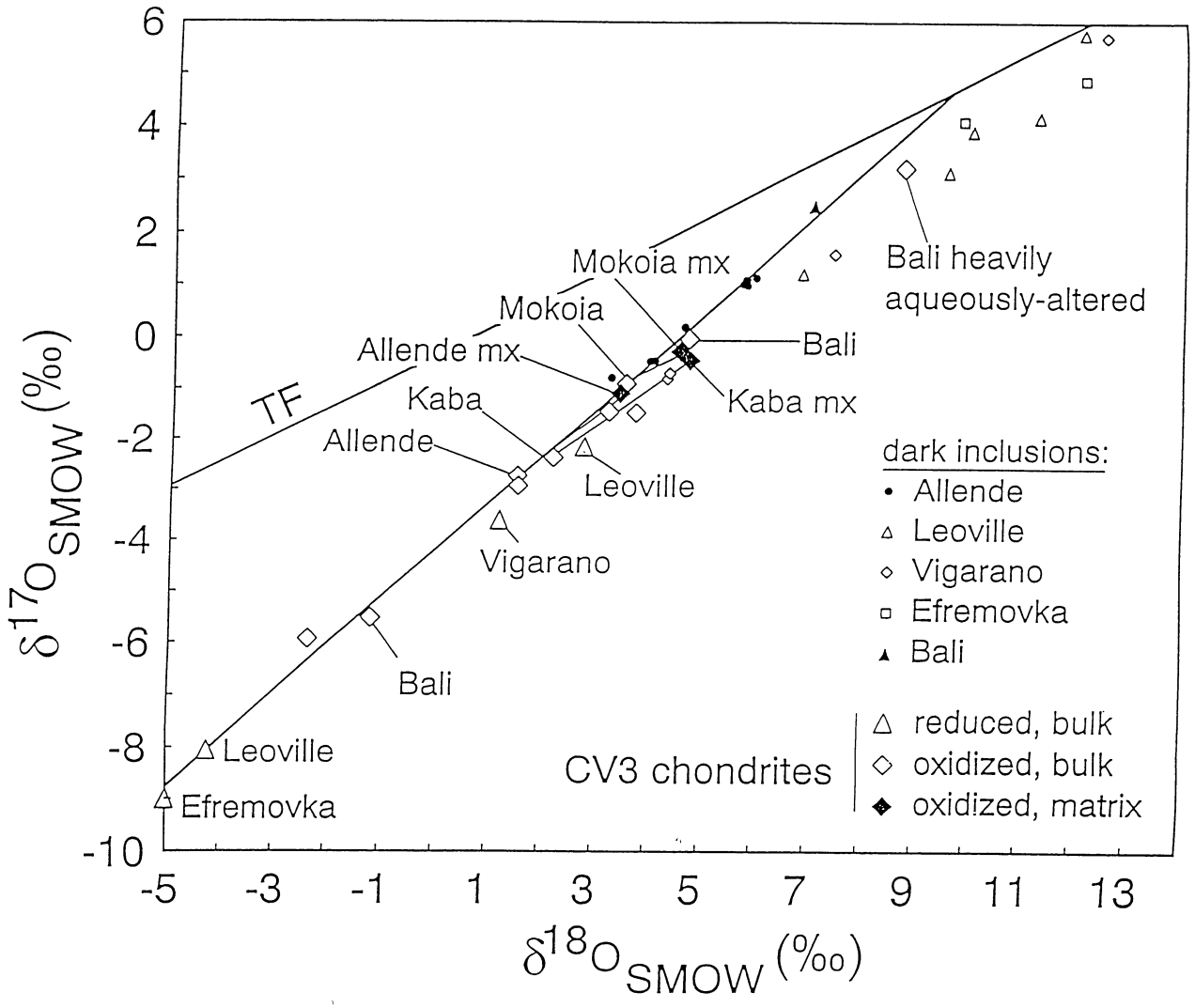

FIG. 14. Bulk O isotopic compositions of CV3 chondrites and their dark inclusions (Clayton and Mayeda, 1984; Clayton *et al.*, 1986, 1987, 1997; Clayton, pers. comm.; Kracher *et al.*, 1985; Keller *et al.*, 1994; Bischoff *et al.*, 1988; Johnson *et al.*, 1990; Krot *et al.*, 1998b; Weisberg *et al.*, 1996). All Allende dark inclusions and one from Bali plot along Allende CAIs line; dark inclusions in the reduced CV3 chondrites Leoville, Efremovka and Vigarano breccia plot to the right of this line. Kaba and Mokoia contain abundant phyllosilicates (Keller and Buseck, 1990; Tomeoka and Buseck, 1990). Matrices in the aqueously altered Kaba and Mokoia, and anhydrous Allende show similar depletions in ^{16}O compared to their hosts. There are significant differences in bulk O isotopic compositions of unaltered and heavily aqueously altered portions of Bali (Keller *et al.*, 1994) and between two analyzed samples of anhydrous Leoville. Some of these variations are probably due to sample heterogeneity. TF = terrestrial fractionation line.